

Modeling Ocular Drift

Janis Intoy

Updated: January 21, 2020

Contents

1	Introduction	3
1.1	General Drift Characteristics	3
1.2	Visual consequences of drift	3
2	Models of Drift	3
2.1	Overview	3
2.2	Brownian Motion	4
2.2.1	Definition	4
2.2.2	Estimating the diffusion constant	5
2.2.3	Properties	5
2.2.4	Empirical Observations	10
2.3	fractional Brownian motion	13
2.3.1	Simulated traces	13
2.3.2	Definition	13
2.3.3	numerical PSD for fractional Brownian motion	17
2.3.4	Properties	21
2.3.5	empirical observations	21
2.4	Ornstein Uhlenbeck process	26
2.5	Model Comparisons	27
2.5.1	R^2 and rmse	28
2.5.2	LR-tests: fBM v BM	30
2.5.3	LR-tests: OUP v BM	32
3	Drift Database & Preprocessing	33
3.1	Data	34
3.2	Procedure & Data Saving	36
4	Empirical estimations of drift PSD	39
4.1	Methods	39
4.1.1	QRad Welch	39
4.2	Other considerations	39
4.2.1	Saturation Regime in Drift - does it exist?	39

4.2.2	Effect of smoothing	40
4.2.3	Effect of sampling frequency	42
5	Appendix	43
5.1	Additional Derivations & Definitions	43
5.1.1	Brownian motion: Diffusion Equation & Solutions	43
5.1.2	PSD of Brownian motion	44
5.1.3	Likelihood ratio testing	45
5.1.4	OUP for small θ is BM	45
5.2	Additional Figures	46
5.2.1	H_{fBM} versus D_{fBM} by task	46
5.3	Data tables	47
5.3.1	Table of Individual Parameters	47
5.3.2	Compare Model Paramaters by Task	50

TO-DO:

1. Look at post-saccadic dynamics of H over drift traces
2. Is smoothed BM a better model of real drifts than unsmoothed BM?
3. Can we predict k_c based on D and H ? Can we tell the difference between changing one parameter or the other? Include graphs of H vs D by task
4. ~~Bug in processing for one of the Fixation5 data set? The fixation period was only 1 second but the traces extend up to 4 seconds? Fixed Jan 19, 2020~~
5. ~~Include example traces with similar D and different H . Added Jan 17, 2020~~

1 Introduction

The purpose of this report is to document knowledge about ocular drift, its properties, and potential models which capture its characteristics (i.e. Janis's journal about drift in general). This is an analysis of ocular drift collected from several studies in the lab. The major questions are:

1. **How Brownian is ocular drift? What other models may describe drift?** Several studies have shown that drift (or more generally fixation) resemble a random walk in that that the variance of displacement grows linearly in time. We do see deviations from this model in individuals but have not thoroughly investigated this question. Engbert and Kleigl (2012?) used a more general model (fractional Brownian motion) to fit the variance of displacement, and found that fixation is persistent (drift away) on a short time scale and anti-persistent (drift centrally) on a long time scale.
2. **How do the characteristics of ocular drift vary with task?** The lab has recorded eye movement traces during a variety of tasks that can be compared. Here we compared their Brownian properties.
3. **Do the characteristics of ocular drift vary within an individual?** We have several subjects who participated in more than one study whose data can be individually compared. (TO-DO)

1.1 General Drift Characteristics

1.2 Visual consequences of drift

2 Models of Drift

2.1 Overview

Here we compare several random walk models of ocular drift characterized by how the variance of displacement of the line of sight varies in time. Note that this section refers to data from the drift-database which are described in detail in Chapter 3.

- Brownian motion (linear): $\langle r^2 \rangle = 4D_{BM}t$

- fractional Brownian motion (power)¹: $\langle r^2 \rangle = 4D_{fBM}t^H$
- Ornstein Uhlenbeck process (exponential): $\langle r^2 \rangle = \frac{2D_{OUP}}{\theta}(1 - \exp(-2\theta t))$

Note that Brownian motion (BM) is a specific case of fractional Brownian motion (fBM) where the Hurst index (H) is 1. ². Engbert and Kliegl use the notation that $H > 1$ is a persistent fixation (accelerating), and $H < 1$ is an anti-persistent fixation. The Ornstein Uhlenbeck process is a random walk in which the variance of displacement asymptotes at a value defined the ratio of its two parameters (D/θ), where θ is inversely related to how quickly the asymptote is reached.

Since BM is a specific case of fBM, these two models can be compared by a likelihood ratio test (LLR; see Section 5.1.3). More generally, the models here are compared by the root mean squared errors or goodness of fit values (R^2).

Note that when θ or t are very small in the OUP model, the variance of displacement can be approximated as linear (for small x , $\exp(x) = 1 + x$). See Appendix ??.

2.2 Brownian Motion

2.2.1 Definition

The probability of gaze location varies with time as

$$\frac{\partial q}{\partial t} = D \frac{\partial^2 q}{\partial x^2} + D \frac{\partial^2 q}{\partial y^2}$$

or equivalently, when $r^2 = x^2 + y^2$ (see Appendix section 5.1.1 for derivation).

$$\frac{\partial q}{\partial t} = \frac{D}{r} \frac{\partial}{\partial r} \left(r \frac{\partial q}{\partial r} \right)$$

The solution to which is $q(x, y, t; D)$. Comparisons are made with the theoretical power spectrum based on Brownian motion drifts, $Q(\xi, f; D)$ - derivation in 5.1.2.

$$q(x, y, t; D) = \frac{1}{4\pi Dt} \exp\left(-\frac{x^2 + y^2}{4Dt}\right)$$

$$Q(\xi_x, \xi_y, f; D) = \frac{2D(\xi_x^2 + \xi_y^2)}{4\pi^2 D^2(\xi_x^2 + \xi_y^2) + f^2}$$

$$Q(\xi, f; D) = \frac{2D\xi^2}{4\pi^2 D^2\xi^4 + f^2}$$

Note that this is often presented in angular frequencies ($k = 2\pi\xi$, $\omega = 2\pi f$) instead of ordinary frequencies (ξ, f):

$$Q(k, \omega; D) = \frac{2Dk^2}{D^2k^4 + \omega^2}$$

¹Note that this is not the standard definition of fBM

²implemented with matlab *fit* with type *exp1* and $\log(t)$ as input. **JI: 2/18/2019** concerned this isn't working because some of the individual LLR test statistics came up negative which shouldn't be possible

2.2.2 Estimating the diffusion constant

For a 2-D isotropic, random walk, we know that

$$\langle r^2 \rangle = \langle x^2 \rangle + \langle y^2 \rangle$$

where $\langle x^2 \rangle = \langle y^2 \rangle = 2Dt$. Therefore,

$$\langle r^2 \rangle = 4Dt \Rightarrow D = \frac{\langle r^2 \rangle}{4t}$$

2.2.3 Properties

Limits of Power

Note that when $D = 0$ there is 0 power at $f \neq 0$. When $D = 0$ and $f = 0$, there is infinite power at all spatial frequencies.

Furthermore, note that when integrating over temporal frequencies to a limit (ideal LPF) the total temporal power is constant and invariant to spatial frequency and diffusion constant.

$$\begin{aligned} \int_0^L Q(\xi, f; D) df &= \left[\frac{1}{\pi} \tan^{-1} \left(\frac{f}{2\pi D \xi^2} \right) \right]_0^L \\ &= \frac{1}{\pi} \tan^{-1} \left(\frac{L}{2\pi D \xi^2} \right) && \text{(log-log linear)} \\ \lim_{L \rightarrow \infty} \int_0^L Q(\xi, f; D) df &= \frac{1}{2} && \text{(constant)} \end{aligned}$$

When integrating over a temporal frequency range (ideal bandpass):

$$\frac{1}{L_2 - L_1} \int_{L_1}^{L_2} Q(\xi, f; D) df = \frac{1}{\pi(L_2 - L_1)} \left(\tan^{-1} \left(\frac{L_2}{2\pi D \xi^2} \right) - \tan^{-1} \left(\frac{L_1}{2\pi D \xi^2} \right) \right)$$

The shape of this function:

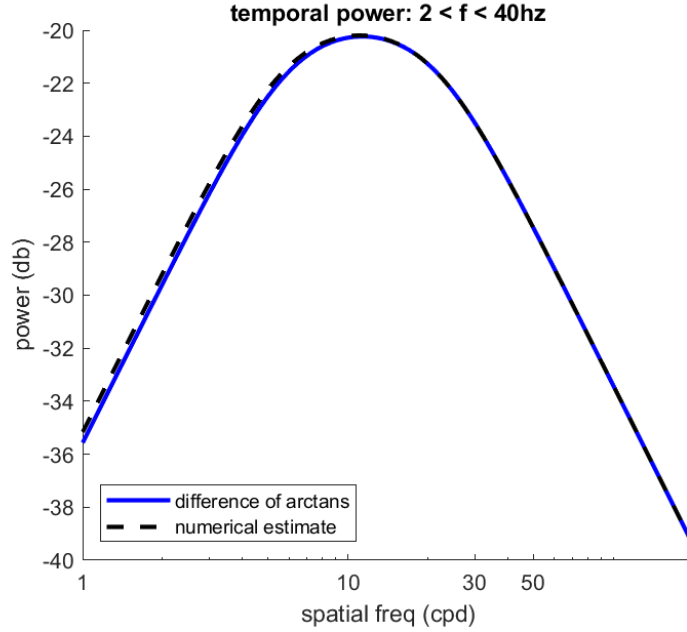


Figure 1: example shape of power vs spatial frequency from ideal bandpass

Impact of D on PSD

Note that for two different retinal diffusion coefficients $D_2 = aD_1$, the resulting spatiotemporal power spectra are spatial frequency-scaled versions of one another:

$$\begin{aligned}
 Q(\xi, f; D_2) &= Q(\xi, f; aD_1) \\
 &= \frac{2D_1 a \xi^2}{4\pi^2 D_a^2 a^2 \xi^4 + f^2} \\
 &= \frac{2D_1 (\sqrt{a}\xi)^2}{4\pi^2 D_a^2 (\sqrt{a}\xi)^4 + f^2} \\
 &= Q(\sqrt{a}\xi, f; D_1)
 \end{aligned}$$

This holds for each individual temporal frequency (see Fig 2) and even after temporal filtering:

$$\begin{aligned}
 S(\xi; D_2) &= \int_0^\infty H(f) Q(\xi, f; D_2) df \\
 &= \int_0^\infty H(f) Q(\sqrt{a}\xi, f; D_1) df \\
 &= S(\sqrt{a}\xi; D_1)
 \end{aligned}$$

where $H(f)$ is the frequency response of some low or bandpass filter. Therefore, the maximum value of $S(\xi; D_2)$ and $S(\xi; D_1) = S(\sqrt{a}\xi; D_1)$ are the same, though the peaks occur at different spatial frequencies for $a \neq 1$.

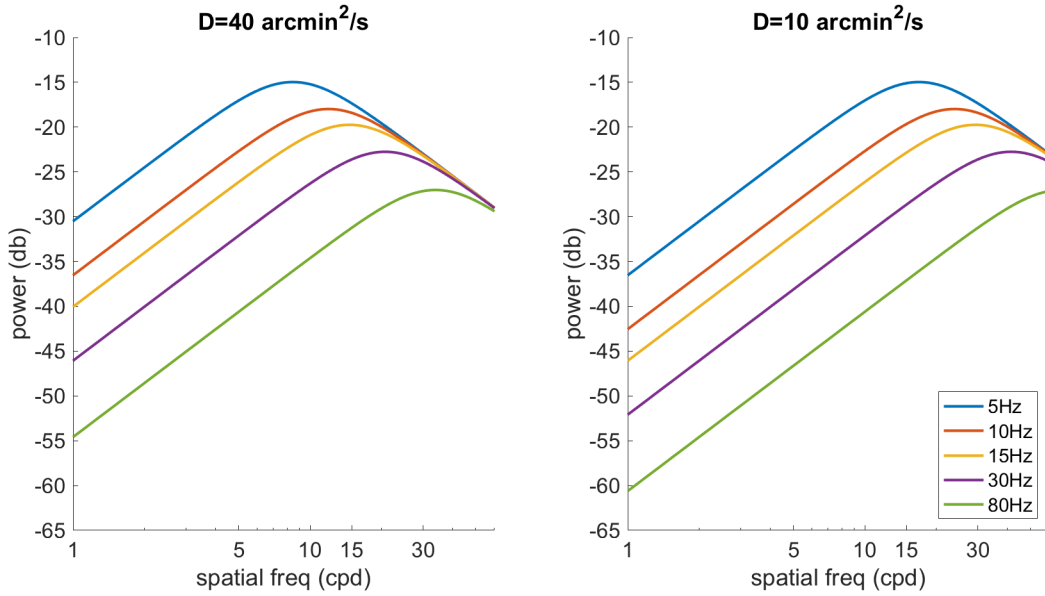


Figure 2: Power in different temporal frequency bands for two diffusion coefficients. Note that changing the diffusion coefficient scales the x-axis so that the the peak values is the same regardless of the diffusion coefficient.

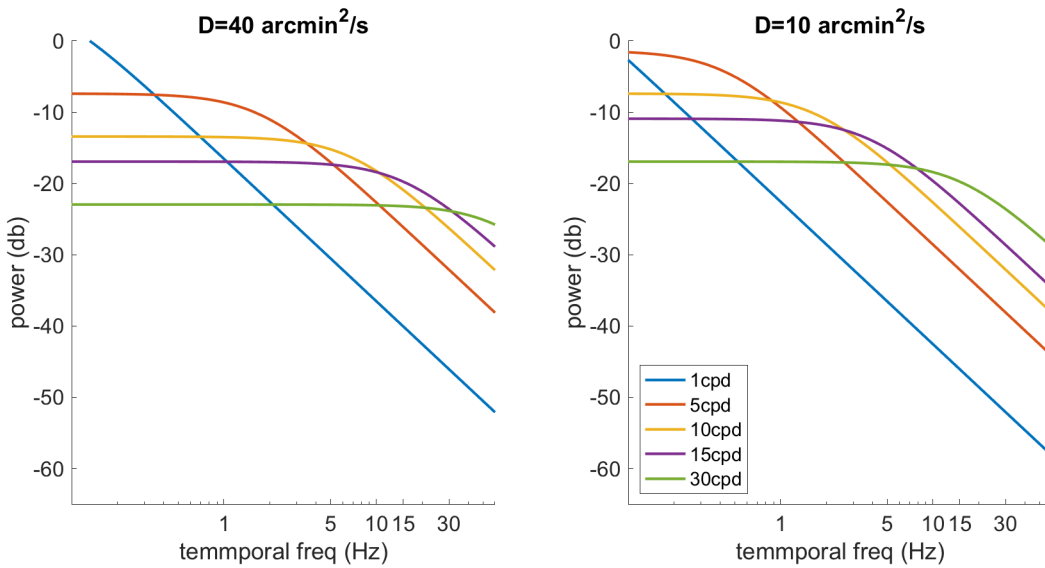


Figure 3: Power in different spatial frequency bands for two diffusion coefficients.

Critical Frequency

Here we compute the spatial frequency at which peak power occurs for a given (f) and show that the value of this peak does not depend on the diffusion constant D .

Given D_R and f :

$$\begin{aligned} \frac{\partial Q}{\partial \xi} = 0 &= \frac{(2^2 D \xi)(2^2 \pi^2 D^2 \xi^4 + f^2) - (2D \xi^2)(2^4 \pi^2 D^2 \xi^3)}{(2^2 \pi^2 D^2 \xi^4 + f^2)^2} \\ &= \frac{(2D \xi)(-2^3 \pi^2 D^2 \xi^4 + 2f^2)}{(2^2 \pi^2 D^2 \xi^4 + f^2)^2} \\ &\Rightarrow 2D \xi = 0 \rightarrow \xi = 0 \quad (\text{minimum}) \\ &\Rightarrow 2^3 \pi^2 D^2 \xi^4 + 2f^2 = 0 \rightarrow \boxed{\xi'^2 = \frac{f}{2\pi D}} \end{aligned}$$

Therefore, we know that power peaks at the spatial frequency $\xi' = \sqrt{f/2\pi D}$ as shown in Figure 4.

Note that when $D = 0$, the power peaks at an infinite spatial frequency so that the power in any temporal frequency band cannot vary and must remain constant at 0 - except at $f = 0$ where power is infinite and constant

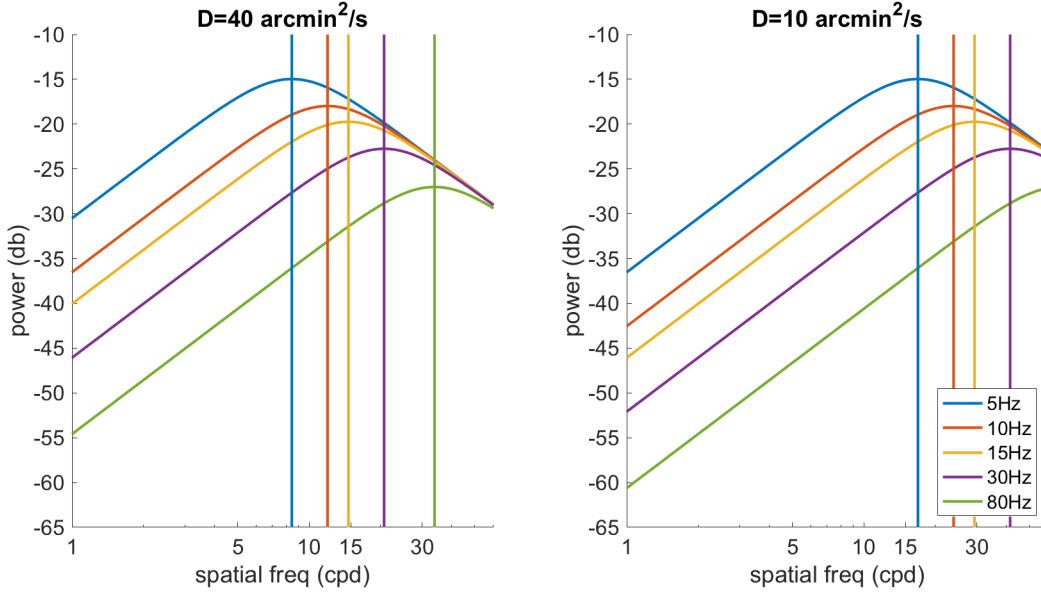


Figure 4: Power in different frequency bands for two diffusion coefficients. Note that changing the diffusion coefficient scales the x-axis so that the the peak values is the same regardless of the diffusion coefficient. The peak location can be predicted as described above.

Given the spatial frequency ξ' at which the peak occurs, we can compute the value of power at this point:

$$\begin{aligned} Q(\xi', f; D_R) &= \frac{2D \frac{f}{2\pi D}}{4\pi^2 D^2 \frac{f^2}{2^2 \pi^2 D^2} + f^2} \\ &= \boxed{\frac{1}{2\pi f}} \end{aligned}$$

Therefore, the peak power in each temporal frequency band is determined only by the temporal frequency (see Figure 5)- and is in fact proportional to the inverse of the temporal frequency.

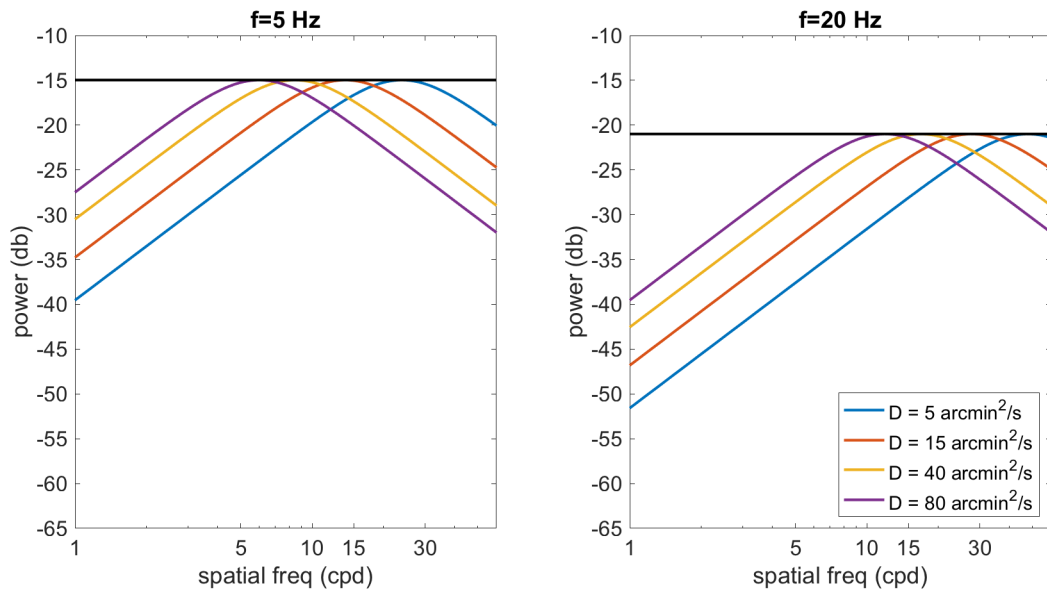


Figure 5: Power for different diffusion constants in two temporal frequency bands. Changing the diffusion constant varies the location of the peak, but the peak value is invariant to the diffusion coefficient.

In log-log-scale, the "stretching" of the spatial frequency axis may appear to be more like a shift. The stretching is more evident when axes are shown in linear scales as shown in Figure 6.

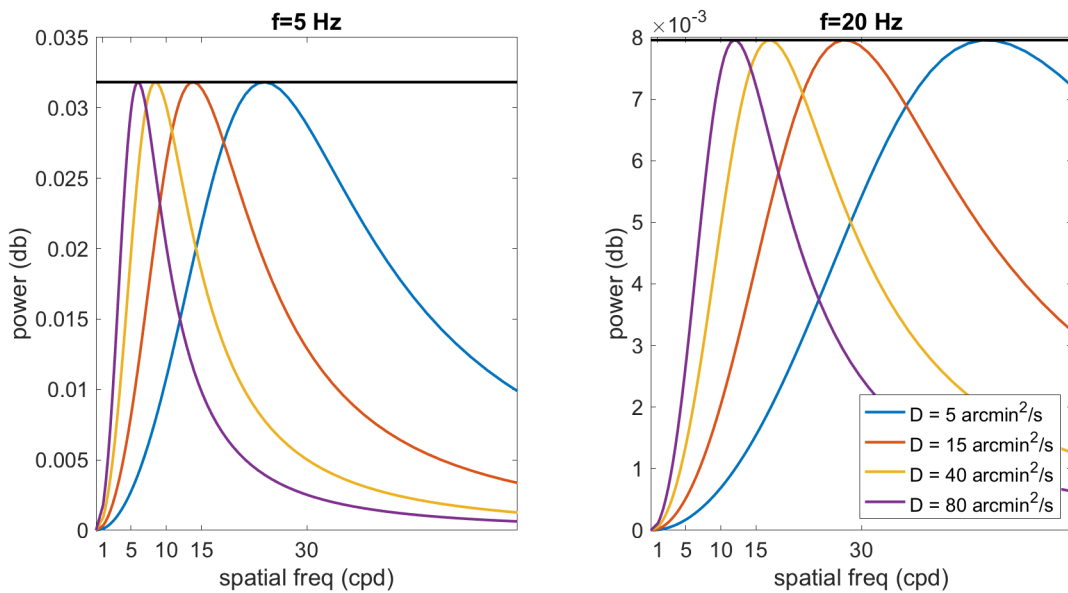


Figure 6: Same as 5 except in linear scale to show stretching of spatial frequency better.

If a temporal filter $H(f)$ is applied, then the power spectrum peaks when: (analogous to above)

$$\begin{aligned} \int H(f) \frac{\partial Q}{\partial \xi} df = 0 &= \int \frac{(2^2 D \xi)(2^2 \pi^2 D^2 \xi^4 + f^2) - (2D \xi^2)(2^4 \pi^2 D^2 \xi^3)}{(2^2 \pi^2 D^2 \xi^4 + f^2)^2} H(f) df \\ &= \int \frac{(2D \xi)(-2^3 \pi^2 D^2 \xi^4 + 2f^2)}{(2^2 \pi^2 D^2 \xi^4 + f^2)^2} H(f) df \\ &\Rightarrow 2D \xi = 0 \rightarrow \xi = 0 \quad (\text{minimum}) \\ &\Rightarrow 2^3 \pi^2 D^2 \xi^4 \int H(f) df + 2 \int f^2 H(f) df = 0 \rightarrow \xi^4 = \frac{\int f^2 H(f) df}{2^2 \pi^2 D^2 \int H(f) df} \end{aligned}$$

Letting $\int H(f) df = 1$, then the integral in the numerator is the second moment of $H(f)$, $h_2 = \int f^2 H(f) df$. Then, the peak value is

$$\begin{aligned} Q(\xi', f; D) &= \frac{2D \frac{\sqrt{h_2}}{2\pi D}}{4\pi^2 D^2 \frac{h_2}{2^2 \pi^2 D^2} + f^2} \\ &= \int \frac{\sqrt{h_2}}{\pi(h_2 + f^2)} H(f) df \end{aligned}$$

2.2.4 Empirical Observations

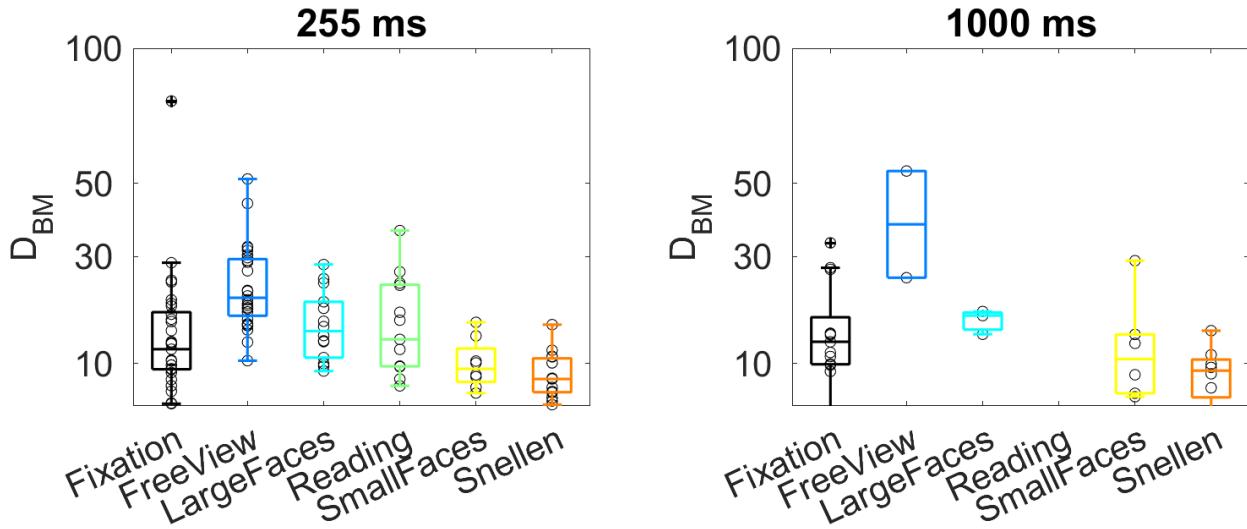


Figure 7: Diffusion constants estimated for each individual and displayed by task on short (left) and long (right) time scales. Individual data are shown by black circles. ANOVA comparison of these values are presented in appendix section 5.3.2

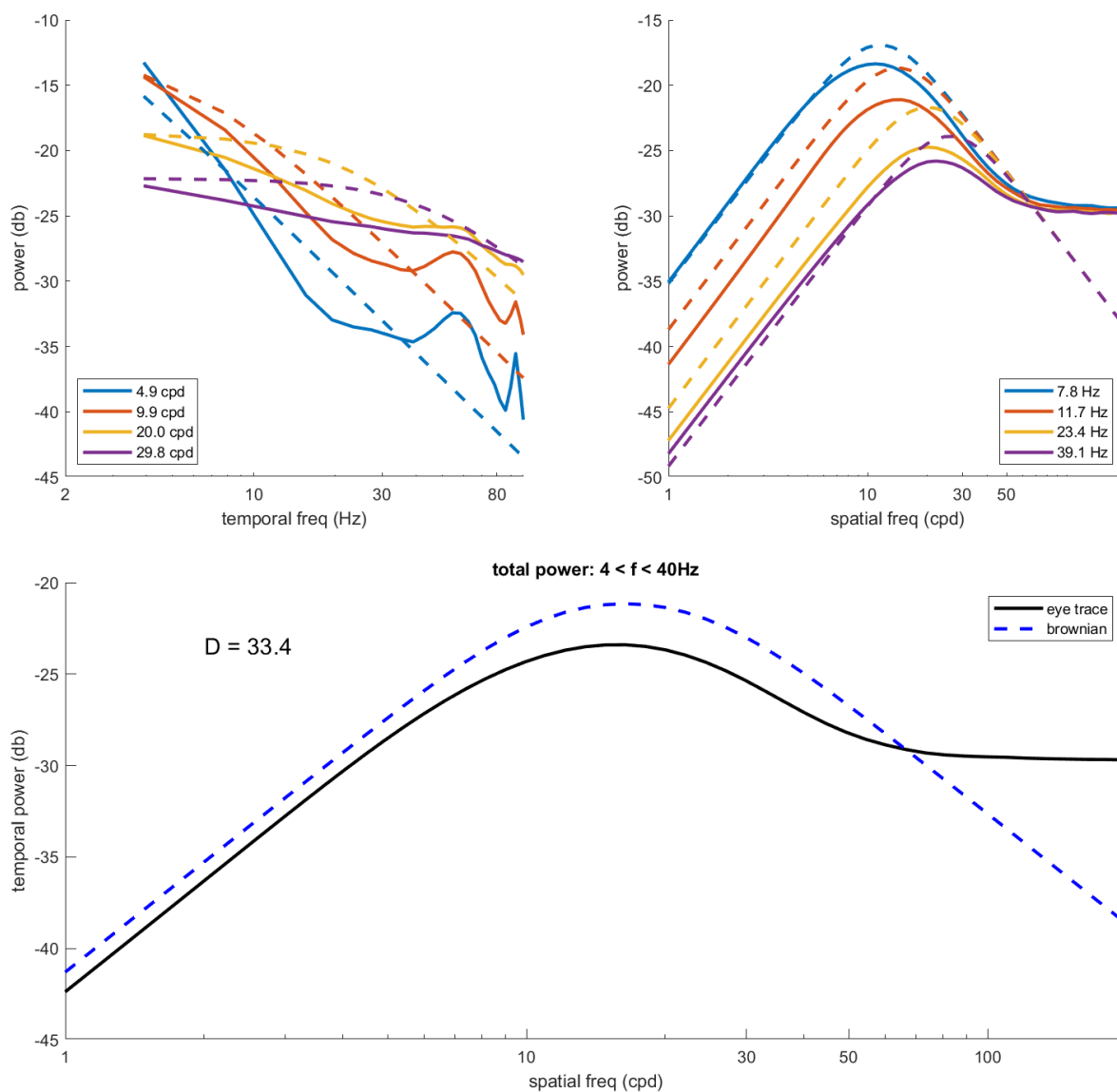


Figure 8: PSD of real drifts (solid curves) and best BM fit (dashed) from Fixation database. LEFT: Slices through a few spatial frequencies. RIGHT: Slices through a few temporal frequencies. BOTTOM: total temporal power between 4 and 40 Hz. Sampling rate 1000 Hz; $nfft = 256$. 50 ms was removed from each of the start and end of the traces. Note that power peaks, drops, then seems to level out starting around 50 cpd where power at all temporal frequencies seem to converge. See PS_QRad.m in DriftCompare folder (Bill.mat).

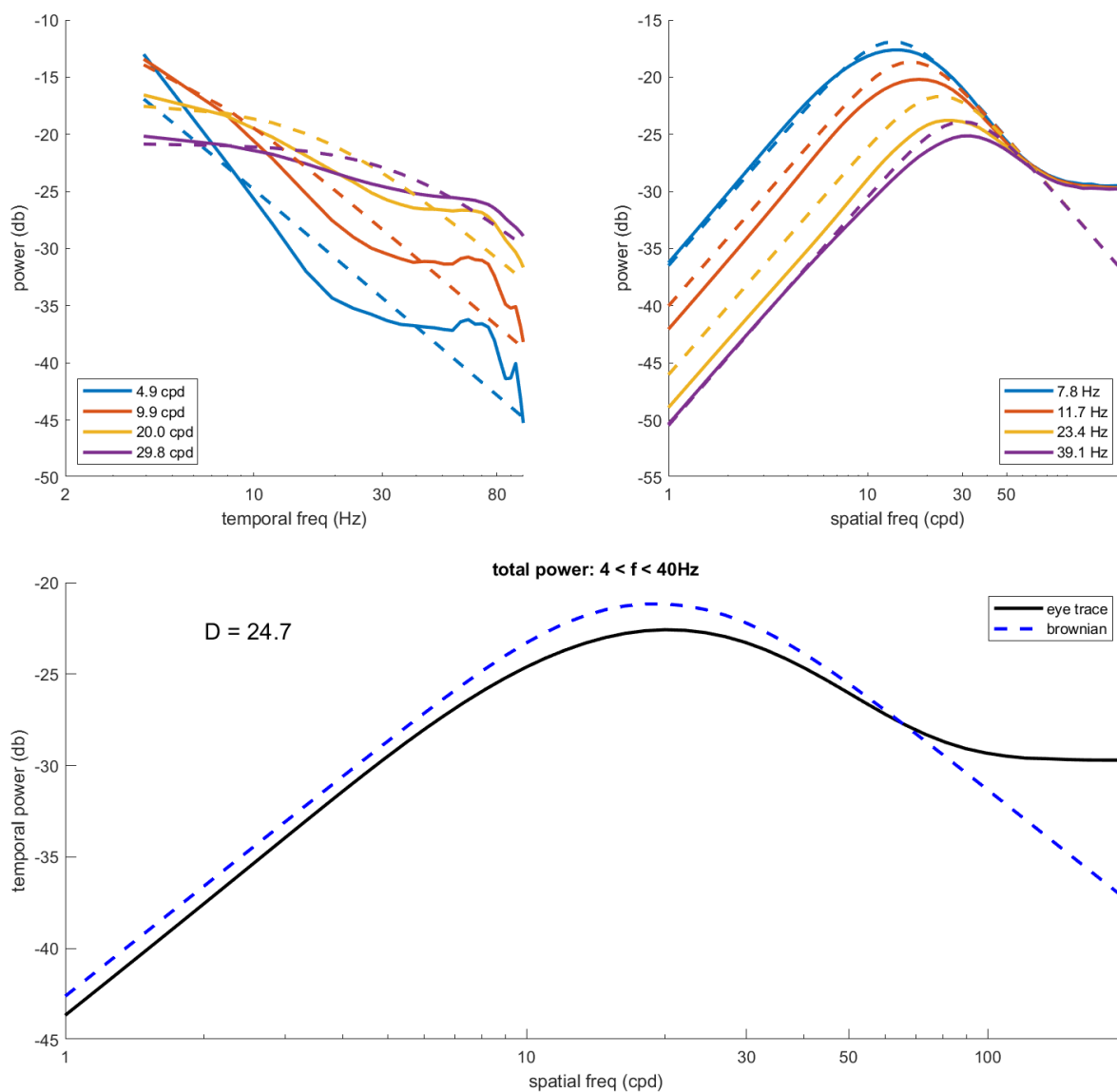


Figure 9: PSD of real drifts (solid curves) and best BM fit (dashed) from Fixation database. LEFT: Slices through a few spatial frequencies. RIGHT: Slices through a few temporal frequencies. BOTTOM: total temporal power between 4 and 40 Hz. Sampling rate 1000 Hz; $nfft = 256$. 50 ms was removed from each of the start and end of the traces. Note that power peaks, drops, then seems to level out starting around 50 cpd where power at all temporal frequencies seem to converge. See PS_QRad.m in DriftCompare folder (David.mat).

2.3 fractional Brownian motion

2.3.1 Simulated traces

fractional Brownian motion is a generalization of brownian motion in which the variance of displacement can vary according to t^H instead of just-linearly. Here is an example of how varying H affects the random walks:

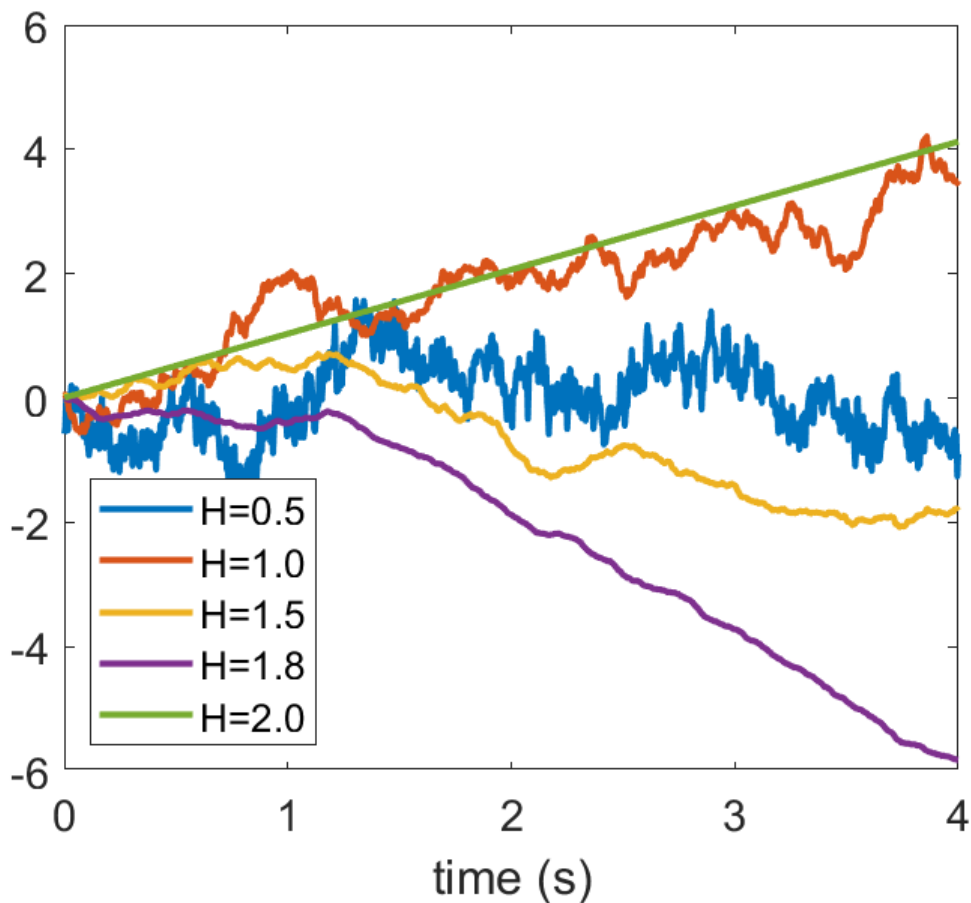


Figure 10: Simulated fBM traces. Note that the $H = 2$ simulation is essentially motion with a constant velocity and direction, though it could randomly also go in the other direction. Using code from mathworks file exchange by Botev - referencing Kroese & Botev (2015) - Spatial Process Simulation.

2.3.2 Definition

The probability of gaze displacement over time with diffusion D is modeled

$$q(x, y, t; D) = \frac{1}{\sigma_t^2 \pi} \exp \left[-\frac{x^2 + y^2}{\sigma_t^2} \right]$$

where $\sigma_t^2 = 4D|t|^H$. The Fourier transform of this in spatial domain is

$$\begin{aligned}\mathcal{F}_{x,y}\{q\}(k_x, k_y, t; D) &= \exp[-\sigma_t^2 \pi^2 (k_x^2 + k_y^2)] \\ &= \exp[-4D|t|^H \pi^2 (k_x^2 + k_y^2)]\end{aligned}$$

Let $k^2 = k_x^2 + k_y^2$, and define \tilde{q} as the partial Fourier transform:

$$\tilde{q}(k, t; D) = \exp[-4D|t|^H \pi^2 k^2]$$

Consider three cases of H when transforming this into the temporal frequency domain ($\mathcal{F}_t\{\tilde{q}(k, t; D)\}$):

1. $H = 0$

In this case, the variance of displacement is constant in time so all power is contained at $f = 0$.

$$\begin{aligned}Q(k, f; D) &= \mathcal{F}_t\{\exp[-4D\pi^2 k^2]\} \\ &= \exp[-4D\pi^2 k^2] \delta(f)\end{aligned}$$

2. $H = 1$

This case is Brownian motion, so the power as shown previously is

$$Q(k, f; D) = \frac{2Dk^2}{4D^2\pi^2 k^4 + f^2}$$

3. $H = 2$

In this case, power in the spatial domain is gaussian in time. Therefore, it also gaussian in temporal frequency.

$$\begin{aligned}Q(k, f; D) &= \mathcal{F}_t\{\exp[-4Dt^2\pi^2 k^2]\} \\ &= \frac{1}{\sqrt{4D\pi k^2}} \exp\left[-\frac{f^2}{4Dk^2}\right]\end{aligned}$$

Note that here the variance of power across temporal frequencies increases with spatial frequency.

However, this definition of power differs from the intuitive version. In the case that $H = 2$, the particle moves with a constant velocity (either negative or positive). Once the particle is moving it will always go in that direction at the speed, so the power of the process should be a fixed line in the frequency domain:

$$\begin{aligned}q(r, t; D) &= \delta(r - 2\sqrt{D}t) \\ \tilde{q}(k, t; D) &= \exp[-4\pi i\sqrt{D}tk] \\ Q(k, f; D) &= \delta(f - 2\sqrt{D}k)\end{aligned}$$

With these definitions, then the total temporal power in a fixed range of frequencies $[L_1, L_2]$ has value $1/(L_2 - L_1)$ for spatial frequencies in the range $\left[\frac{L_1}{2\sqrt{D}}, \frac{L_2}{2\sqrt{D}}\right]$.

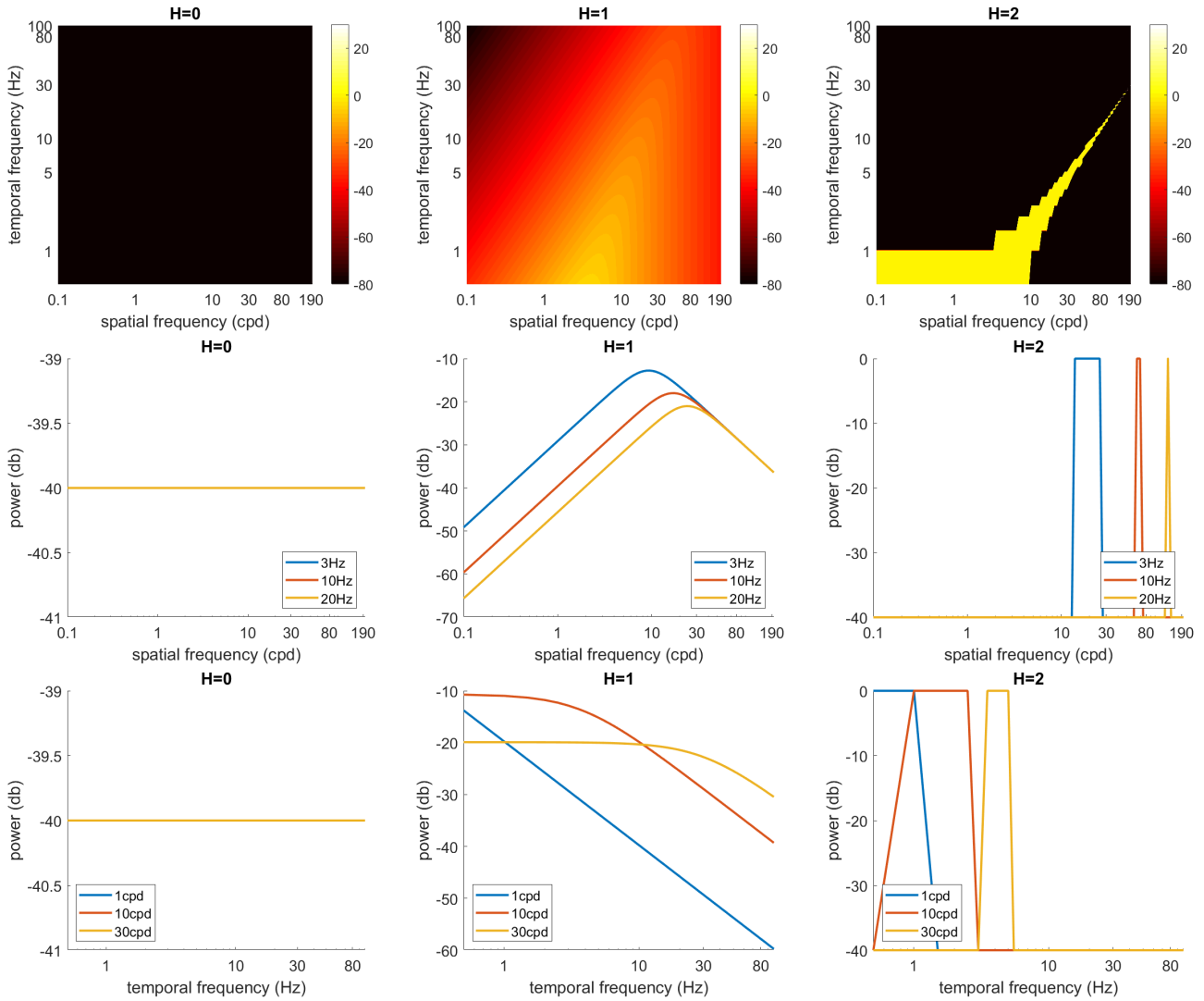


Figure 11: TOP ROW: Power spectral densities for fixed diffusion ($D = 20\text{arcmin}^2/\text{s}$). MIDDLE ROW: slices across temporal frequencies. BOTTOM ROW: slices across spatial frequencies. We already know that spatial whitening occurs in the $H = 1$ case as power increases with k^2 . This whitening effect seems to vanish by $H = 2$ where power is contained entirely along a line in the spatiotemporal frequency domain. (see plotQfBM.m in DriftCompare folder)

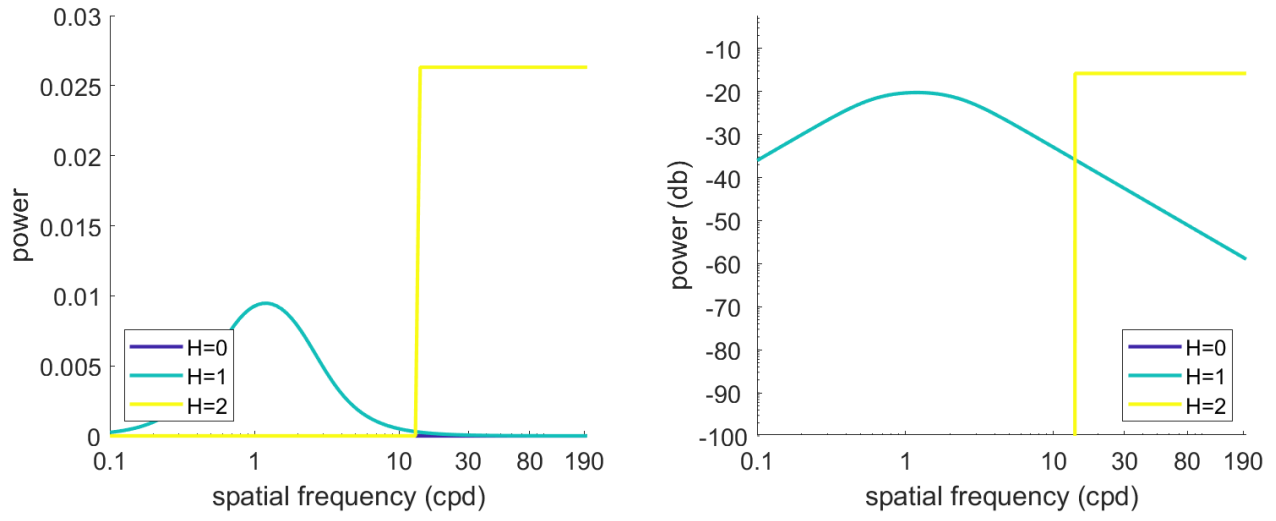


Figure 12: Total temporal power for $2 \leq f \leq 40\text{Hz}$ (computed from closed form definite integrals). Note that temporal power for $H = 2$ is non-zero only in a certain range of spatial frequencies.

2.3.3 numerical PSD for fractional Brownian motion

Section 2.3.2 describes closed-form PSD for only a few cases of fractional Brownian motion, but we are interested in the power spectra for intermediate cases of H as well. We can evaluate this numerically by evaluating the FFT of $\tilde{q}(k, t; D)$ defined above.

Calculations below were done with the following parameters:

- sampling frequency = 2^{10}
- $t \in [-30, 30]$ seconds
- $D = 20$ arcmin²/s

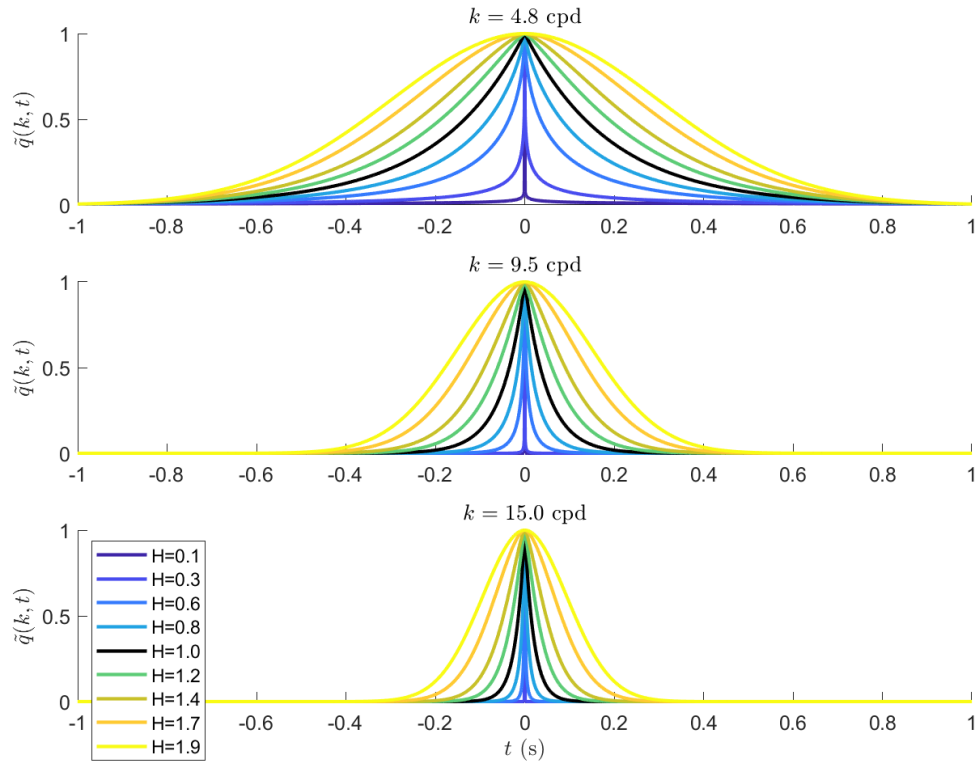


Figure 13: Sample $\tilde{q}(k, t; D)$ as a function of time for several spatial frequencies (k) and Hurst indices (H). Transform these over time to numerically compute $Q(k, f; D)$.

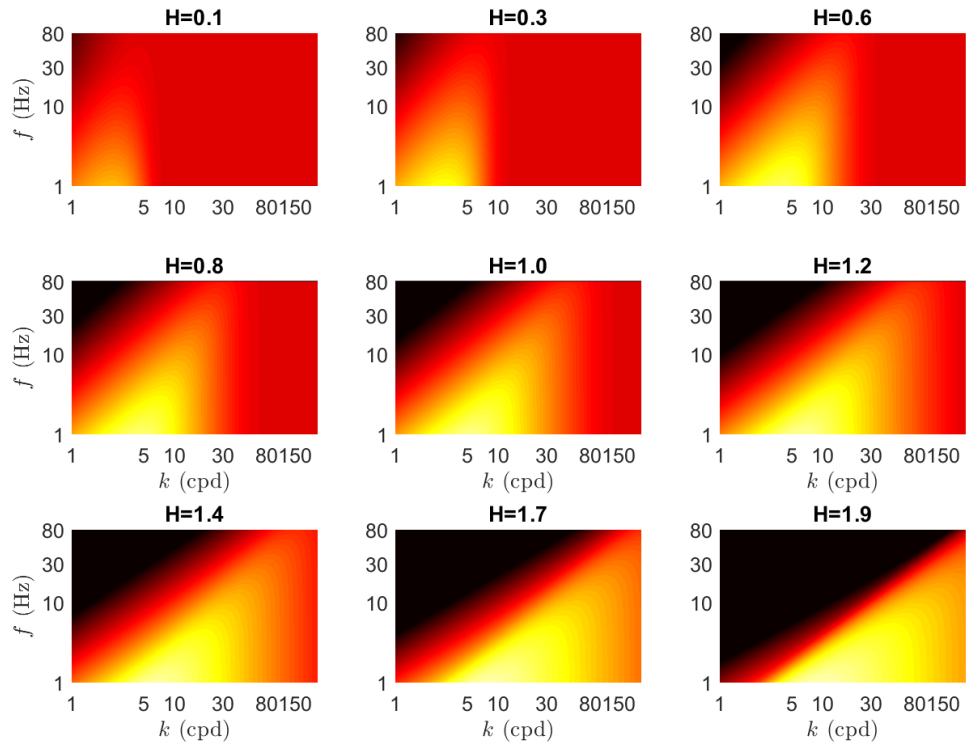


Figure 14: Power spectra $Q(k, f; D)$ for several Hurst indices (H). (Color axes are the same in all panels.)

We can evaluate how well the whitening effect occurs in each of these conditions by computing the temporal power

$$S(k; D) = \int Q(k, f; D) T(f) df$$

For convenience here we use $T(f) = 1$ for $f \in [2, 40]$ and 0 otherwise.

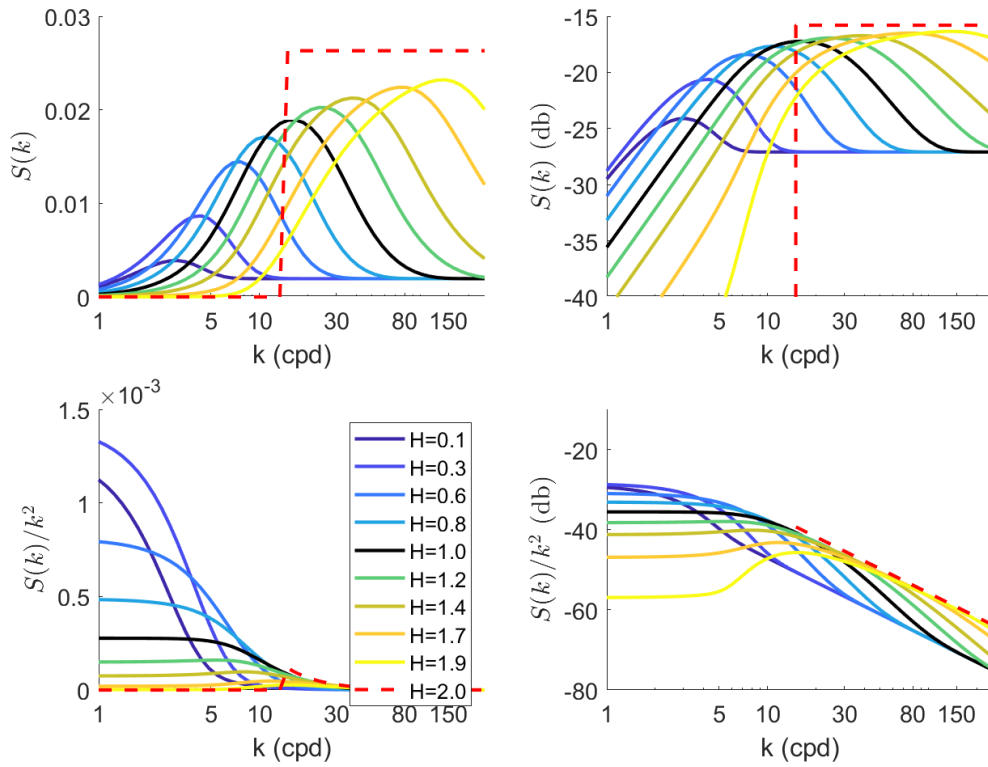


Figure 15: Temporal power $S(k; D)$ (TOP ROW) and normalized by squared spatial frequency $S(k; D)/k^2$ (BOTTOM ROW) for several Hurst indices (H). Whitening occurs for all $H < 2$ - however there is an interesting “bump” at high spatial frequencies for H near 2 (for example, in the bottom right panel $H = 1.8$ case, there is an increase in power starting around 6 cpd). Increasing H pushes the critical frequency up and increases the value of peak power, and decreases the power at lower spatial frequencies. Note that $H = 2$ was computed analytically here. $D = 20$ arcmin²/s.

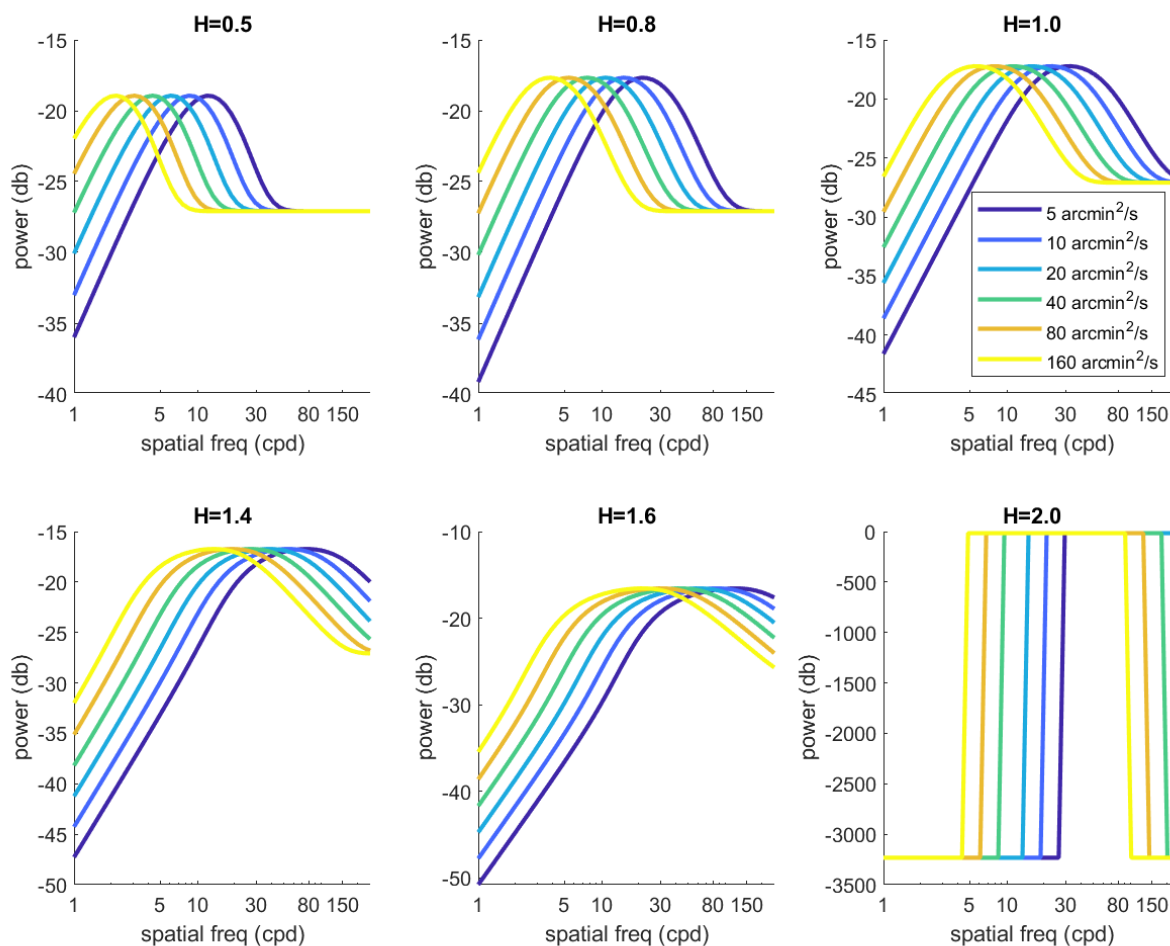


Figure 16: Effect of changing D on $S(k; D)$ for fixed H . The increased power at high H and low D is an artifact of the numerical process. As with BM, changing D appears to shift the spectra along the spatial frequency axis. Note that $H = 2$ here was computed analytically and is shown for comparison.

2.3.4 Properties

2.3.5 empirical observations

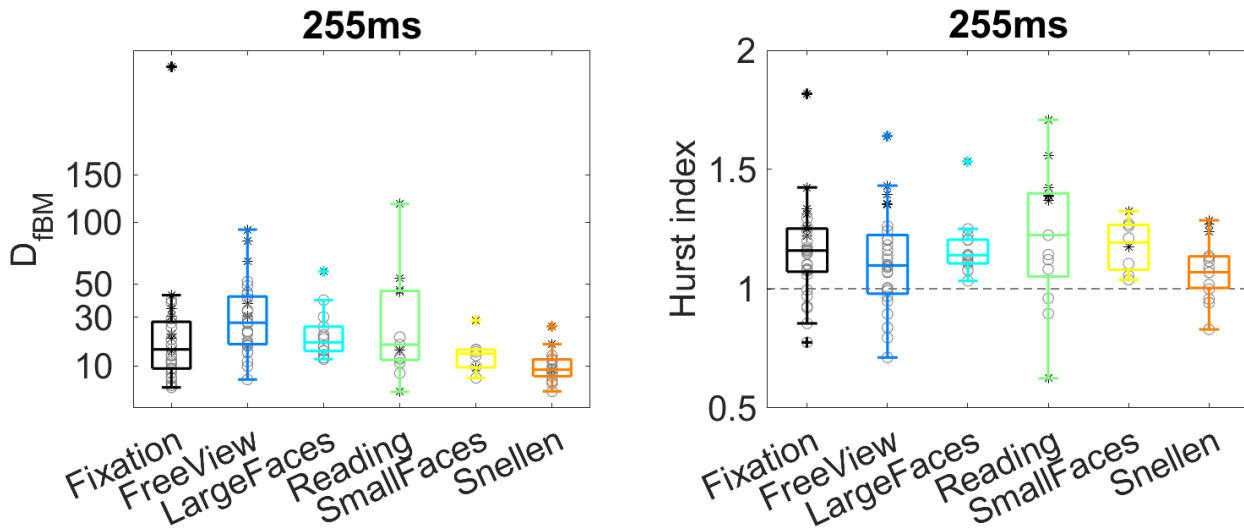


Figure 17: Fractional diffusion constants and hurst indices estimated for each individual and displayed by task on the [short](#) time scale. Individual data are shown by black stars if the fractional BM model was a significantly better fit to the $\langle r^2 \rangle$ data ($p < .05$, likelihood ratio test). A large proportion of the Fixation and FreeView and Reading data seem to resemble fractional brownian motion. ANOVA comparison of these values are presented in appendix section 5.3.2

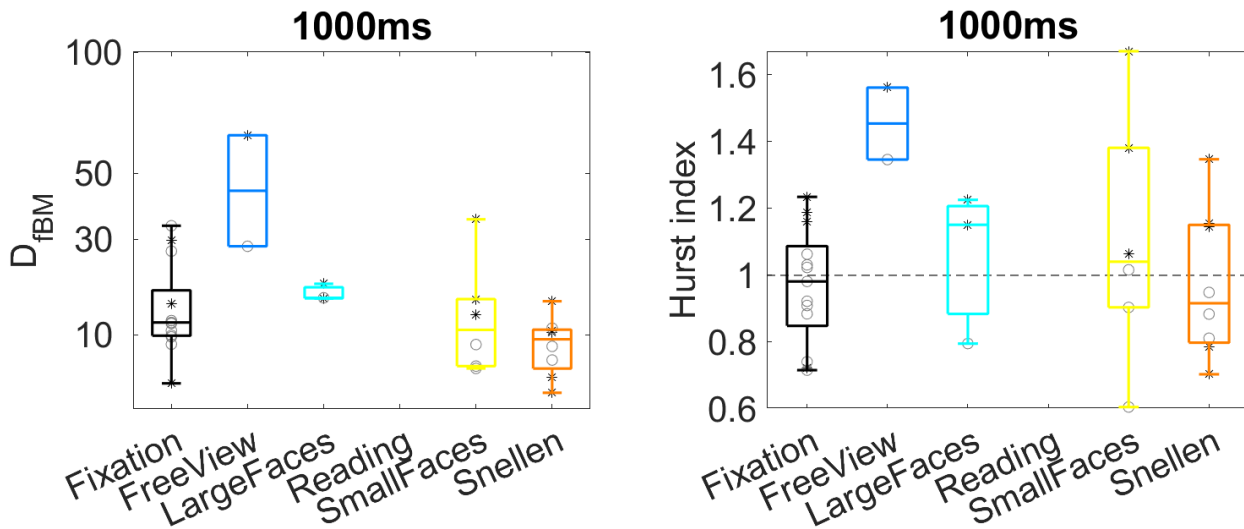


Figure 18: Fractional diffusion constants and hurst indices estimated for each individual and displayed by task on the [long](#) time scale. Individual data are shown by black stars if the fractional BM model was a significantly better fit to the $\langle r^2 \rangle$ data ($p < .05$, likelihood ratio test). A large proportion of the Fixation and FreeView data seem to resemble fractional brownian motion. ANOVA comparison of these values are presented in appendix section 5.3.2

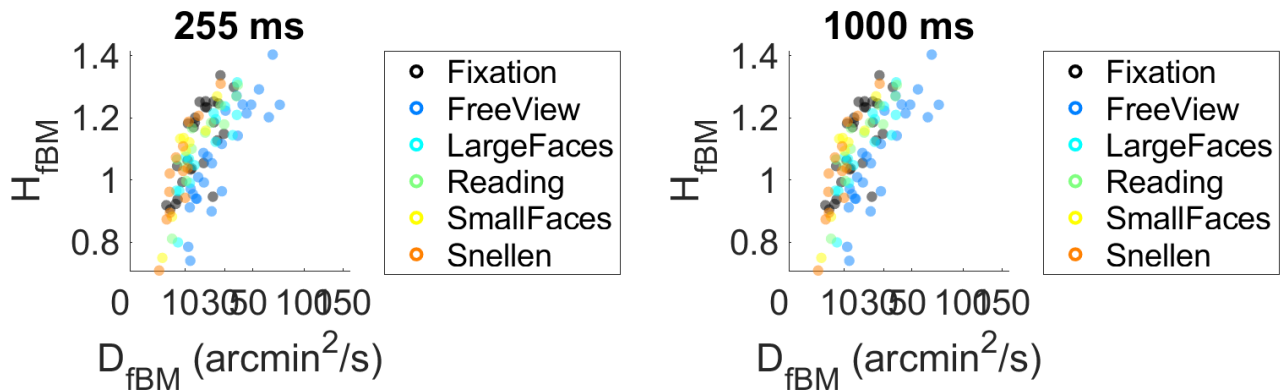


Figure 19: Hurst index versus D_{fBM} for each subject colored by task. Note the correlation between D_{fBM} and H_{fBM} . Since larger D push the critical frequency up and large H drop the critical frequency, these effects may act to cancel each other out. This plot is broken out by task in section 5.2.1.

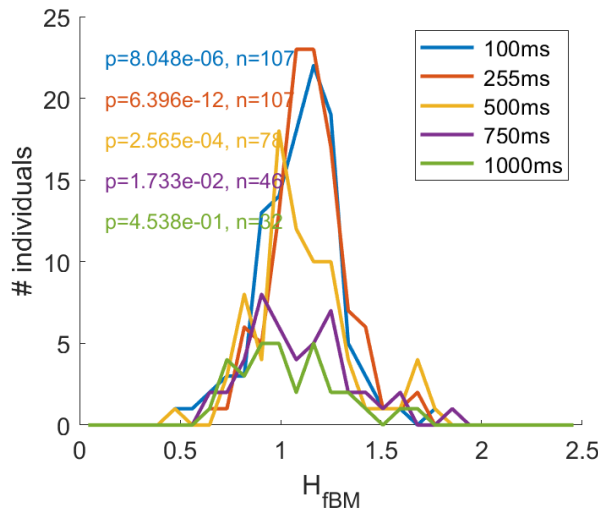


Figure 20: Dynamics of fBM with length of fixation. Distributions of Hurst index when fBM is fit to different time delays across all tasks. Note how the mode of the distribution shifts towards 1 (Brownian motion) with increasing fixation duration. Since $H = 1$ is a signature of BM, a one-sample t -test was run to compare the mean of each distribution to 1 (p -values shown in top left corner). Means and standard deviations of each are listed in the first table of section 5.3.1.

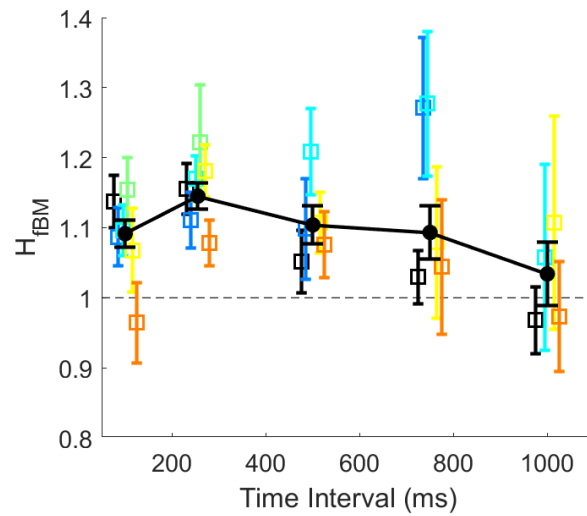


Figure 21: Dynamics of H_{fBM} with length of fixation. Graph shows means and SEM across all individuals (solid black circles) and broken down by task (colored squares with same color legend as in Figure 7). This value does not seem to trend over time, and changes are within the error of the estimates. Snellen (orange) is consistently closer to 1 than other tasks though. Means and standard deviations of each are listed in the first table of section 5.3.1.

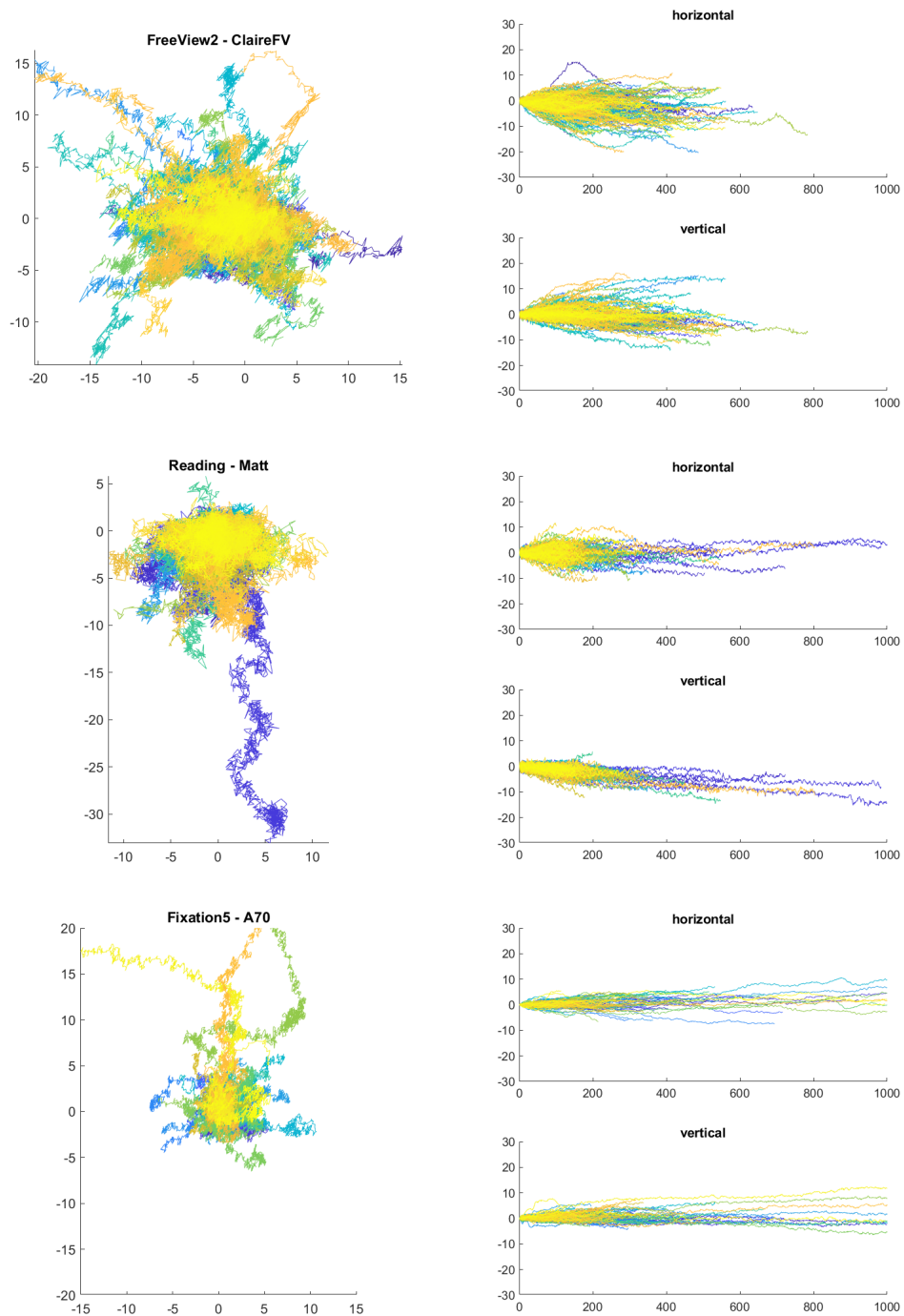


Figure 22: Sample eye traces of subjects with similar D but different H . TOP: $D = 44.32$ and $H = 1.20$. MIDDLE: $D = 44.63$ and $H = 1.37$. BOTTOM: $D = 49.59$ and $H = 1.75$. Note that from top to bottom, there are more traces that go directly away from the initial position. (JI: Note that the Fixation5-A70 traces here included what appeared to be a smooth pursuit portion of the trial)

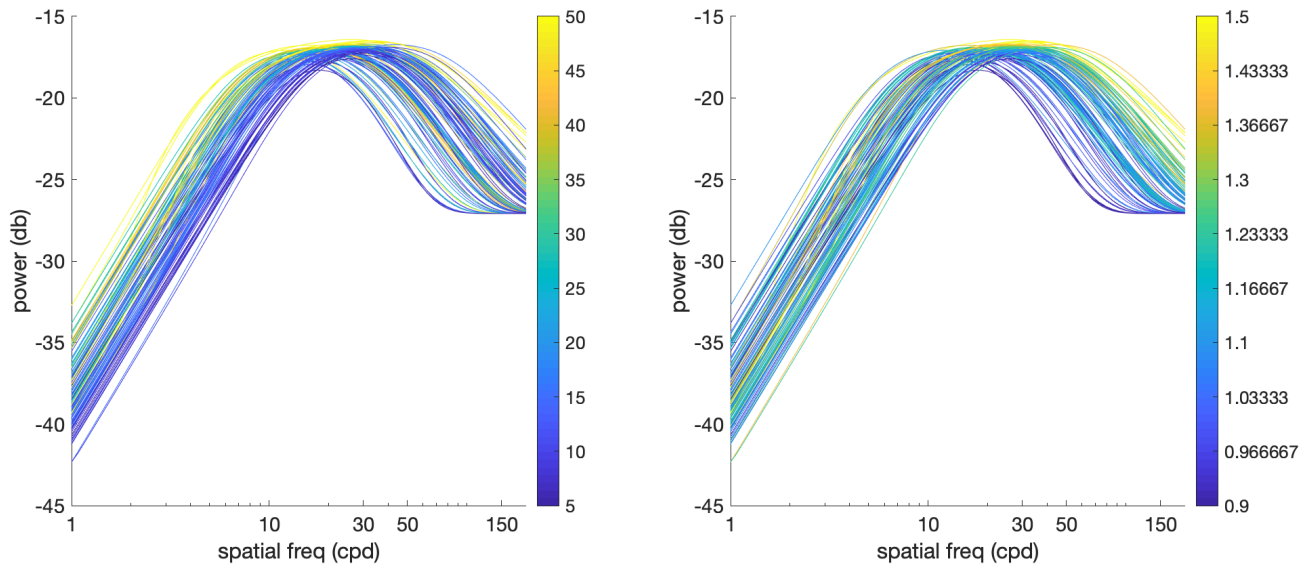


Figure 23: $S(k; D, H)$ based on empirically-observed parameters D and H . Individual lines show individual observers, here colored by diffusion constant (left panel) or Hurst index (right panel). Note that the power spectra are visibly separable by both parameters, so the correlation between them do not completely cancel each other out (under these conditions). See numeralPSD_fBM.m in DriftCompare folder.

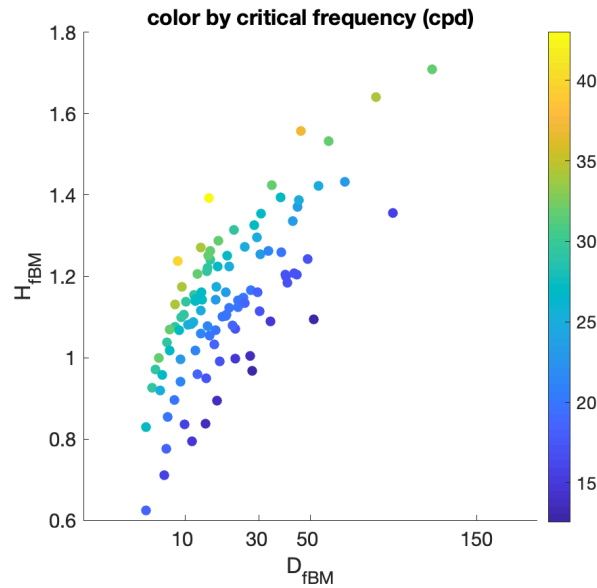


Figure 24: H_{fBM} versus D_{fBM} colored by the critical spatial frequency based on $S(k; D, H)$. Note that the critical frequency is highest for individuals lying along the upper edge.

2.4 Ornstein Uhlenbeck process

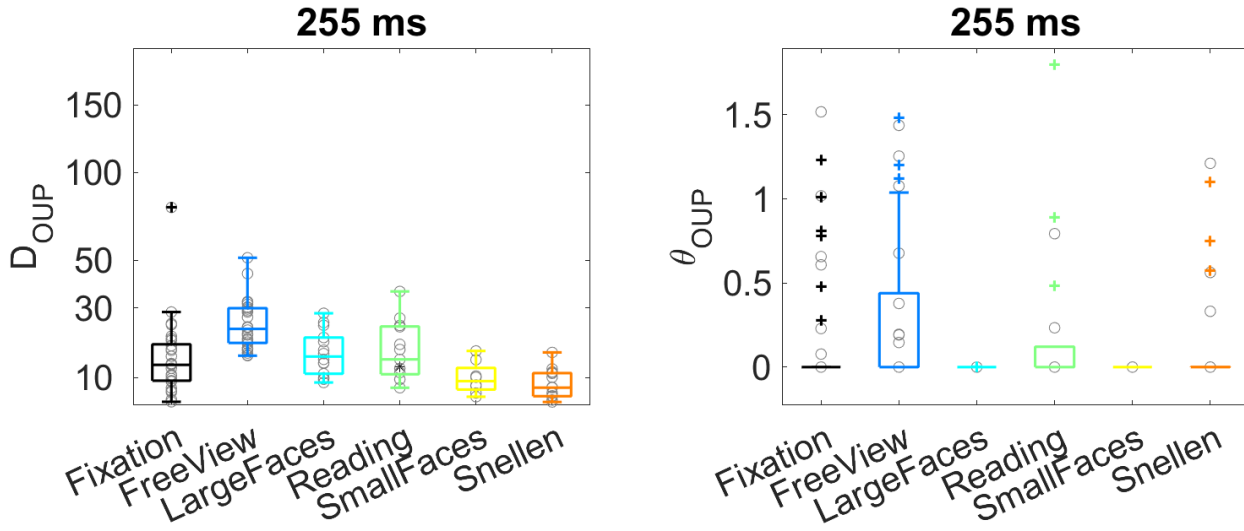


Figure 25: OUP model parameters estimated for each individual and displayed by task on the [short](#) time scale. Individual data are shown by gray circles. Note how most θ values floor at 0, suggesting a linear model would be sufficient.

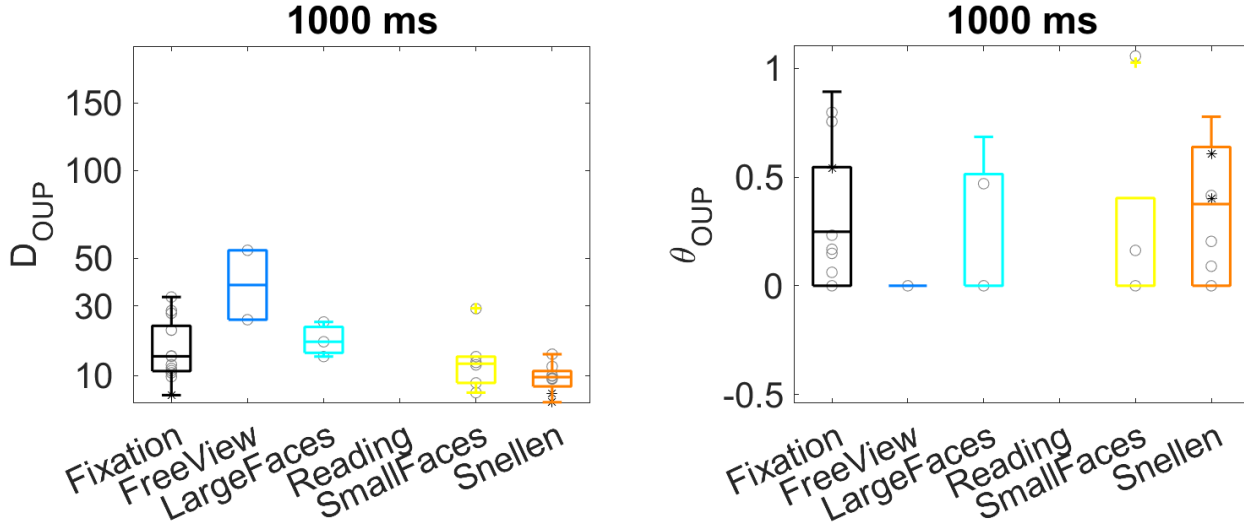


Figure 26: OUP model parameters estimated for each individual and displayed by task on the [long](#) time scale. Individual data are shown by gray circles. Note how many θ values floor at 0, suggesting a linear model would be sufficient. Snellen appears to be the most like an OUP, especially at the longer time interval.

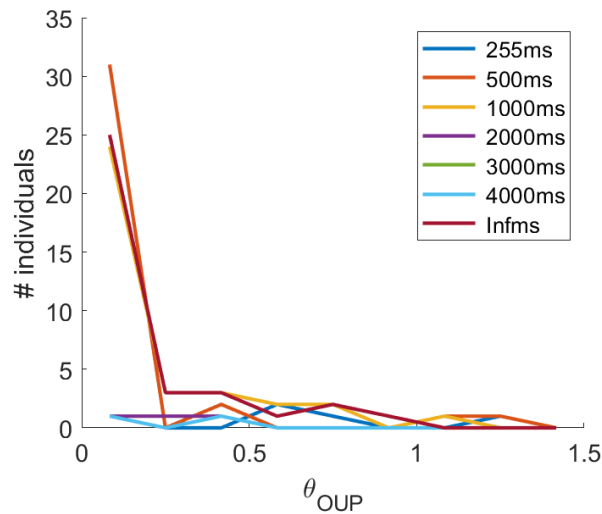


Figure 27: Dynamics of OUP with length of fixation. Distributions of θ_{OUP} when fBM is fit to different time delays across all tasks. Note how the mode of the distribution shifts towards 0 (Brownian motion) with decreasing fixation duration. Means and standard deviations of each are listed in the first table of section 5.3.1.

2.5 Model Comparisons

General observation: The fractional brownian motion model best fits the empirical variances of displacement as shown by the adjusted R^2 and rmse values below. However, fBM provides a significant improvement in the model in a small proportion of individuals, shown by the likelihood tests (see ??).

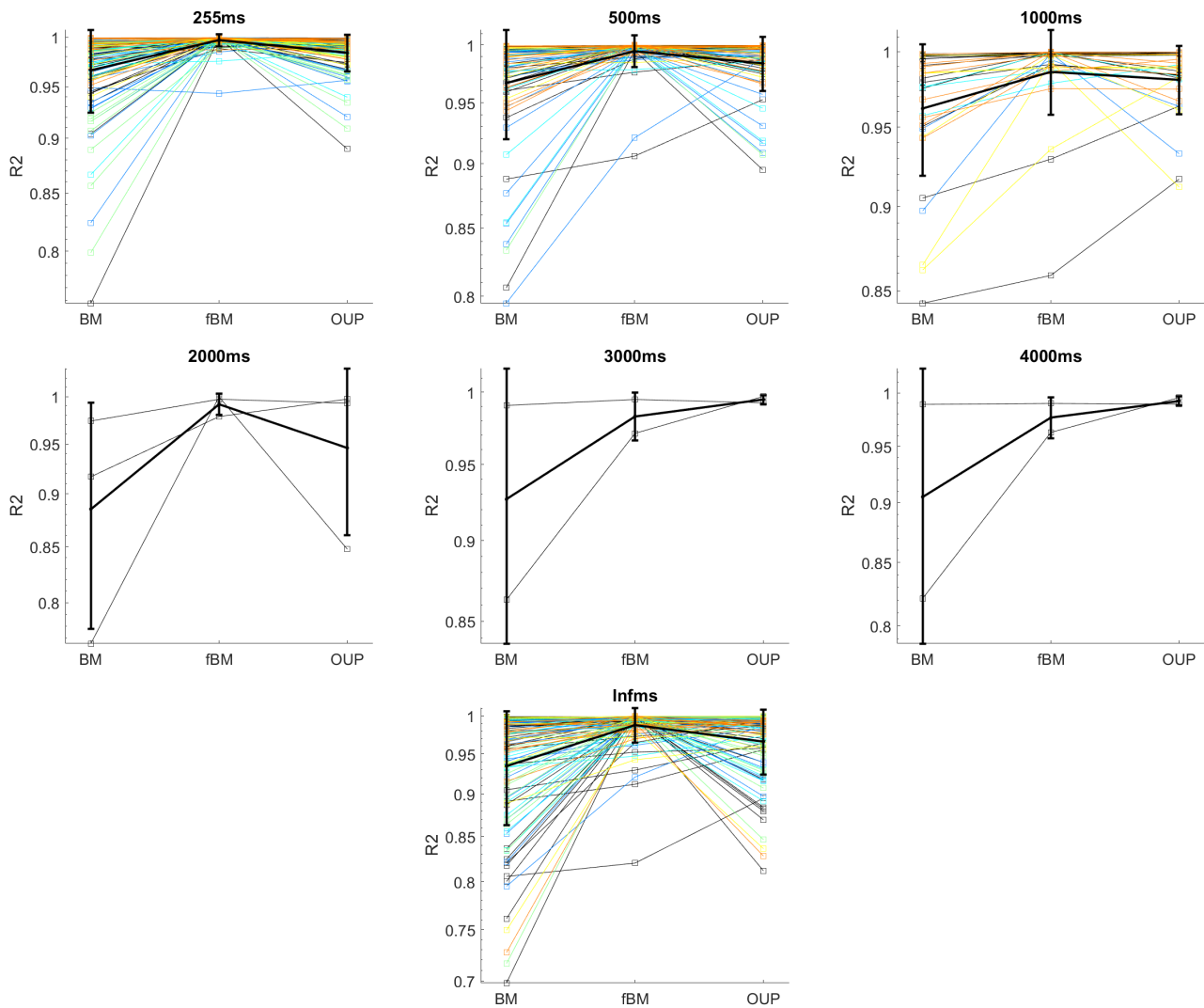
2.5.1 R^2 and rmse

Figure 28: Adjusted R^2 goodness of fit of each model at different time scales. Overall, fractional Brownian motion best fits the empirical data. The adjusted R^2 takes into account the number of parameters in the model (one for BM, two each for fBM and OUP)

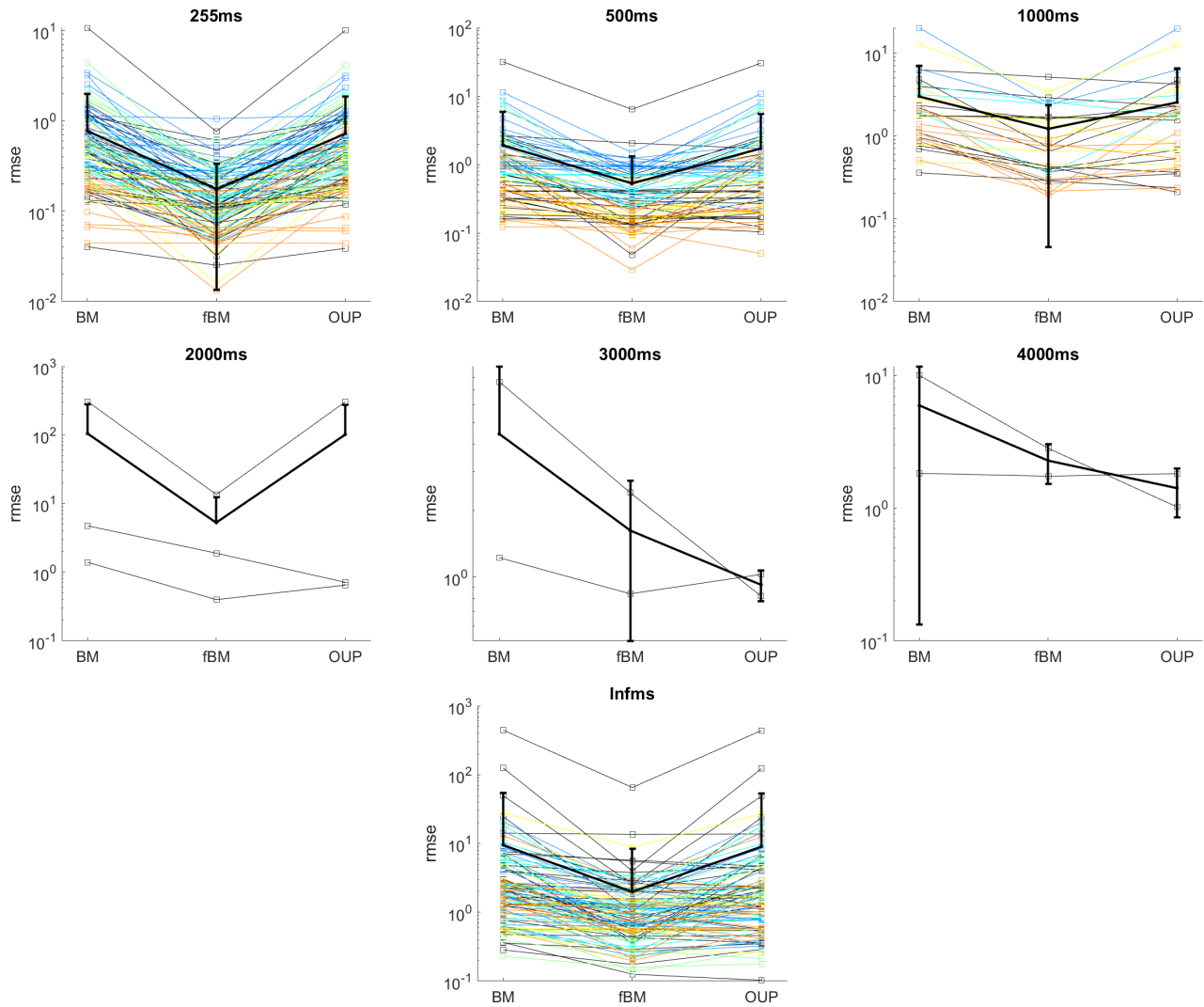


Figure 29: root mean squared error of each model at different time scales. Overall, fractional Brownian motion best fits the empirical data.

2.5.2 LR-tests: fBM v BM

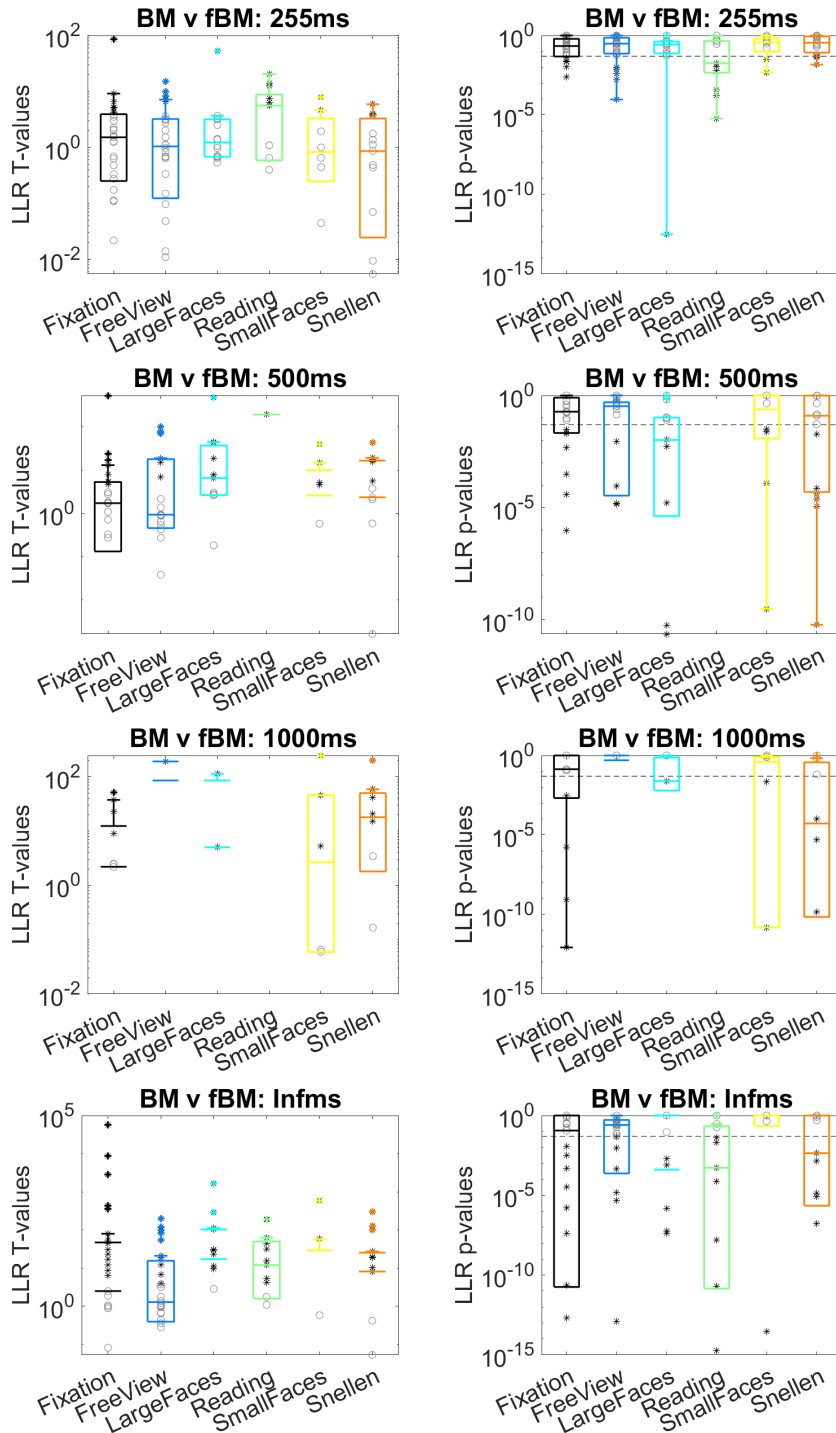


Figure 30: The log-likelihood test statistic (T-val, left) and corresponding p-values (right) comparing fBM and BM. Black starred points indicate a significant p-value (that fBM is a better than BM).

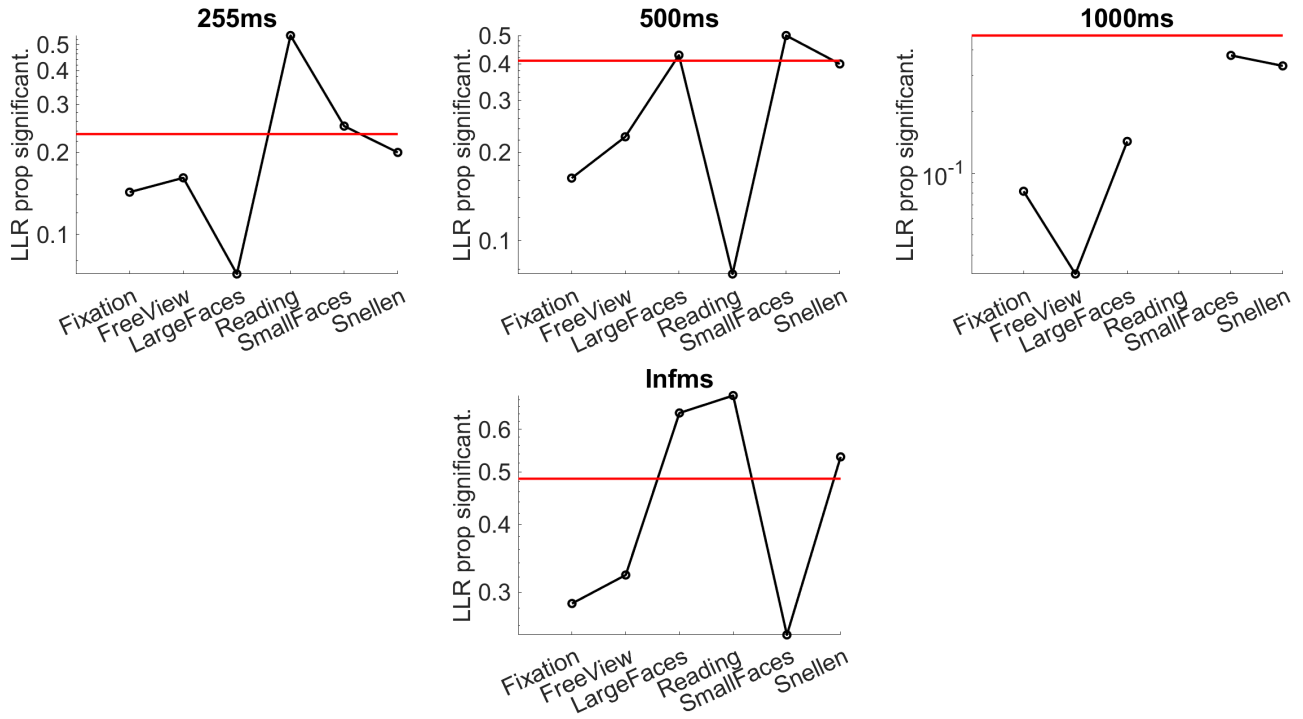


Figure 31: Proportion of individuals for whom fBM is a significantly better fit than BM.

2.5.3 LR-tests: OUP v BM

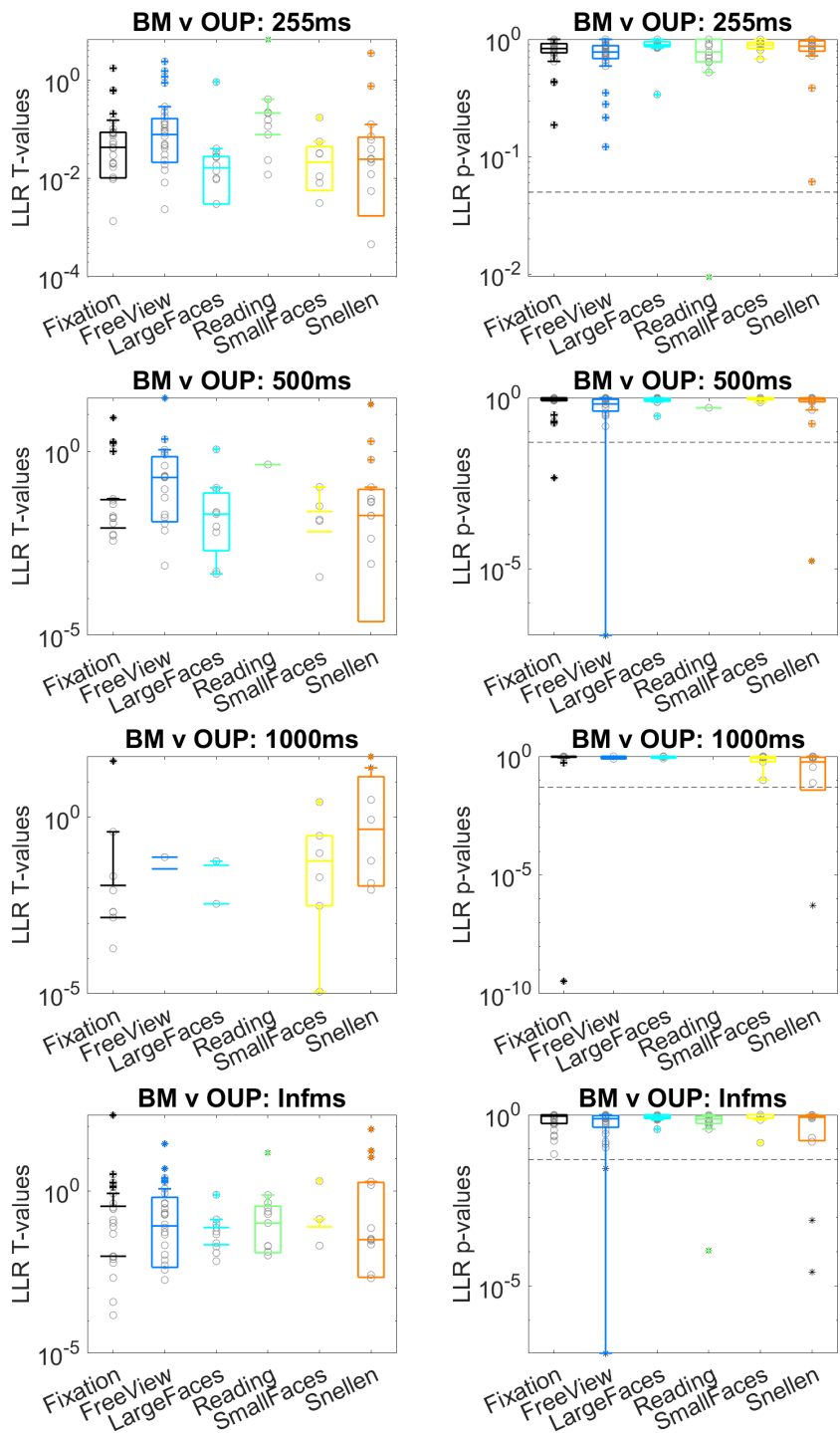


Figure 32: The log-likelihood test statistic (T-val, left) and corresponding p-values (right) comparing OUP and BM. Black starred points indicate a significant p-value (that OUP is a better than BM).

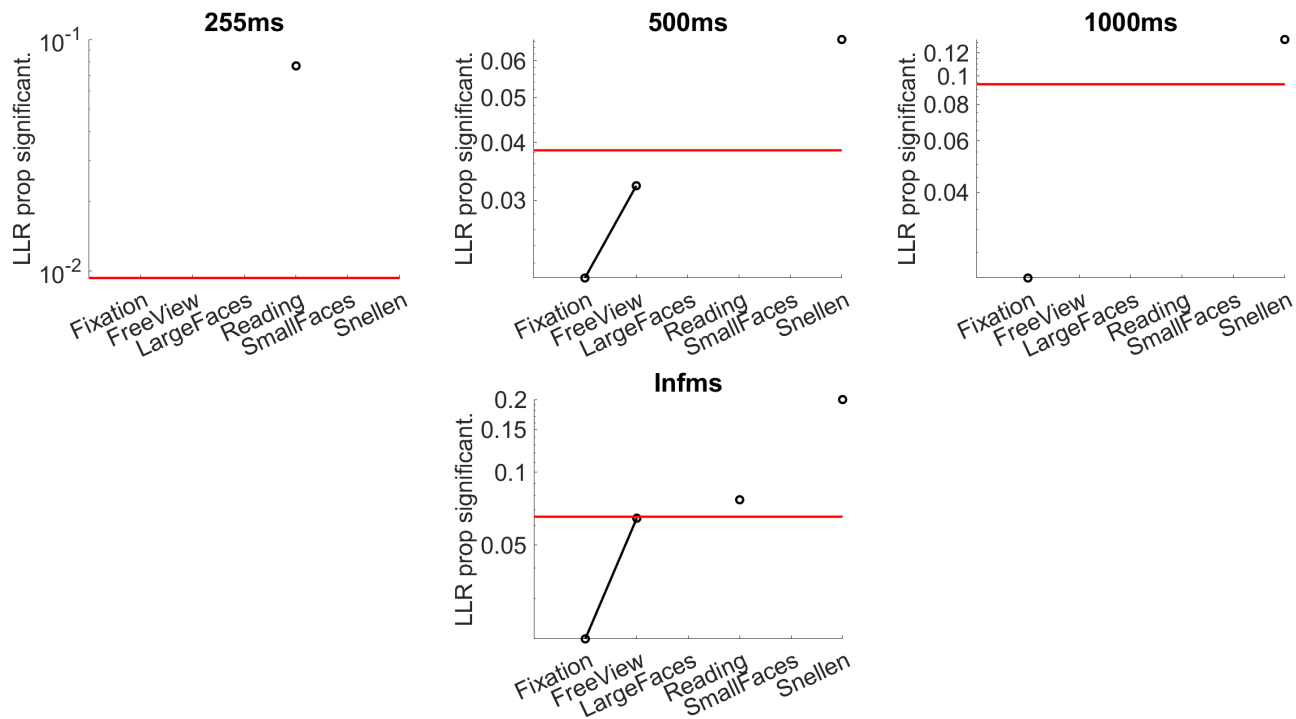


Figure 33: Proportion of individuals for whom OUP is a significantly better fit than BM.

3 Drift Database & Preprocessing

- Analysis Code: <https://gitlab.com/jintoy/DriftCompare>
- Data: Reformatted versions are on BOX (ask Janis), but all data were originally pulled from OPUS, many from BACKUPS. See tables in Section 3.1 for more details.

3.1 Data

Task	# Subjects	Description
Fixation	54	sustained fixation - usually with a marker
FreeView	32	free viewing of natural images
LargeFaces	15	expression discrimination of large faces - 5 deg height? (Shelchkova et al)
SmallFaces	10	expression discrimination of small faces - 1 deg height? (Shelchkova et al)
Reading	14	reading task (Bowers et al, 2018)
Snellen	8	20/20 line eye chart discrimination
1-2cpd	13	1-2cpd grating orientation discrimination
4-5cpd	4	4-5cpd grating orientation discrimination
8-10cpd	11	8-10cpd grating orientation discrimination
12-16cpd	13	12-16cpd grating detection or orientation discrimination

Table 1: Major task categories and the number of subjects (not necessarily unique) that participated in each.

Table 2 (below): Breakdown of major tasks into data sets. Janis’s copy of data along with original data locations (TO-DO) are also listed. Some data were already broken up into fixation structures (“preprocessed”) so I’m not sure if they were filtered, trimmed, ...

Task	#	Description	BOX source	original
Fixation				
Fixation	12	Cherici et al (2012), marker on, 5s(?) fixations	/FixationPrecision/Data	ClaudiaProjects/FixationPrecision/Data/
Fixation2	15	Shelchkova et al (Large Faces - fixation trials)	/Faces/LargeFaces	BACKUPS/Shelchkova.Backup/Christie-MSFaces/Data
Fixation3	10	Shelchkova et al (Small Faces - fixation trials)	/Faces/SmallFaces/Processed	BACKUPS/Shelchkova.Backup/
Fixation4	14	Bowers & Poletti (2017) - fixation trials	/Reading/data	BACKUPS/Bowers.Backup/Reading/data/
Fixation5	8	Snellen monocular fixations (800-1000ms)	/Snellen/Processed	JanisData/APLab/EyeChartE_Stuff
FreeView				
FreeView	10	Drift Gain (Bowers) with gain = 1, 30sec trials	/DriftGain_FreeView	BACKUPS/Bowers.Backup/DriftGain/FreeView
FreeView2	21	FreeView database from OPUS	/FreeViewingDatabase	FreeViewingDatabase
LargeFaces				
LargeFaces	15	Shelchkova et al, 2s(?) trials	/Faces/LargeFaces	BACKUPS/Shelchkova.Backup/Christie-MSFaces/Data
SmallFaces				
SmallFaces	10	Shelchkova et al, 2s(?) trials	/Faces/SmallFaces/Processed	BACKUPS/Shelchkova.Backup/
Reading				
Reading	14	Bowers & Poletti (2017)	/Reading/data	BACKUPS/Bowers.Backup/Reading/data/
Snellen				
Snellen	8	Snellen monocular data, self-paced trials	/Snellen/Processed	JanisData/APLab/EyeChartE_Stuff
1-2cpd				
1cpd	4	Christie CS data, 1.5s trials with contrast ramp and plateau	/ContrastSensitivityData/1cpd	BACKUPS/Poletti.Backup/Martina/Contrast
2cpd	4	Christie CS data, 1.5s trials with contrast ramp and plateau	/ContrastSensitivityData/2cpd	BACKUPS/Poletti.Backup/Martina/Contrast
1cpd2	4	Boi et al (2017) - one-over-f exp, preprocessed	/exp_one_over_f/1cpd	BACKUPS/Boi.Backup/projects/coarse_to_fir
1cpd3	5	Mostofi et al (2016), preprocessed	/DriftTraces_CP_ThTTrials/1cpd	BACKUPS/Mostofi.Backup/backup_Sept2016 codes and data/Data/CleanData/DriftDb/DriftTraces_C
4-5cpd				
4cpd	4	Christie CS data, 1.5s trials with contrast ramp and plateau	/ContrastSensitivityData/4cpd	BACKUPS/Poletti.Backup/Martina/Contrast
5cpd	4	Christie CS data, 1.5s trials with contrast ramp and plateau	/ContrastSensitivityData/5cpd	BACKUPS/Poletti.Backup/Martina/Contrast
8-10cpd				
8cpd	4	Christie CS data, 1.5s trials with contrast ramp and	/ContrastSensitivityData/8cpd	BACKUPS/Poletti.Backup/Martina/Contrast

3.2 Procedure & Data Saving

The following is implemented in *runAll.m*.

- Individuals with less than 20 valid drift segments were removed from analysis.
- Drifts during stimulus presentation were extracted from the data.
- Shorter trials (generally <5s) with blinks and no-tracks during stimulus presentation were removed from analysis. In longer trials, only drift periods occurring within 200ms of a blink or no-track segment were removed from analysis.
- Drift periods with durations <100ms were removed from analysis. The first and last 50ms of each drift period were also discarded.
- Diffusion constants were estimated on the remaining drift periods for each individual in each task. The regression period excludes the first 50ms of time lag.
- Janis's processed data are saved on BOX: <https://rochester.app.box.com/folder/65801521764>
 - Subfolders: dsq255-2 ($\langle r^2 \rangle$ computed up to 255ms lag - a fast data set) and dsq_long ($\langle r^2 \rangle$ computed up to the longest duration possible for each individual - a very slow dataset)
 - .mat files are created for each individual in each task (Task_Subject.mat) and contains the following:
 - * *fix* struct array : each element contains the x and y traces of a drift segment. The structure may contain additional information if created by the original experimenter.
 - * *data* struct with characteristics about each drift in fix:
 - subject: subject name or source file name of vt cell array
 - task: (str) minor label
 - keepBlinks: (bool) whether or not trials with blinks were kept
 - driftIndex: (vector) if available, trial index from vt of corresponding drift segment
 - duration: (vector) duration of each corresponding drift segment (before trimming)
 - curvature: (vector) average curvature of each corresponding drift segment
 - speed (vector): average speed of each corresponding drift segment (computed with `sgfilt`, `smoothing = 41`)
 - varHorz and varVert: (vectors) positional variance of each drift segment
 - span: (vector): radius of smallest circle that contains each drift
 - diffCoeff: (double): diffusion constant estimated from all drift segments (recomputed in post-processing)
 - Dsq: (vector) $\langle r^2 \rangle$ that was used for diffusion constant estimation
 - DsqSingleSeg: (array) $\langle r^2 \rangle$ for each individual drift segment
 - FracBM: currently not computed (done in post-processing)
 - diffCoeffBoot: bootstrap iteration computations of diffusion constant
 - FracBMBoot: currently not computed (done in post-processing)

· dsqBoot: bootstrap iteration computations of Dsq

The main outcome of this processing is the empirical variances of displacement over time for each individual. These can be used downstream to fit different models and estimate diffusion constants. Images of different time scales are shown in Section ???. Individual variances are shown in Section ???.

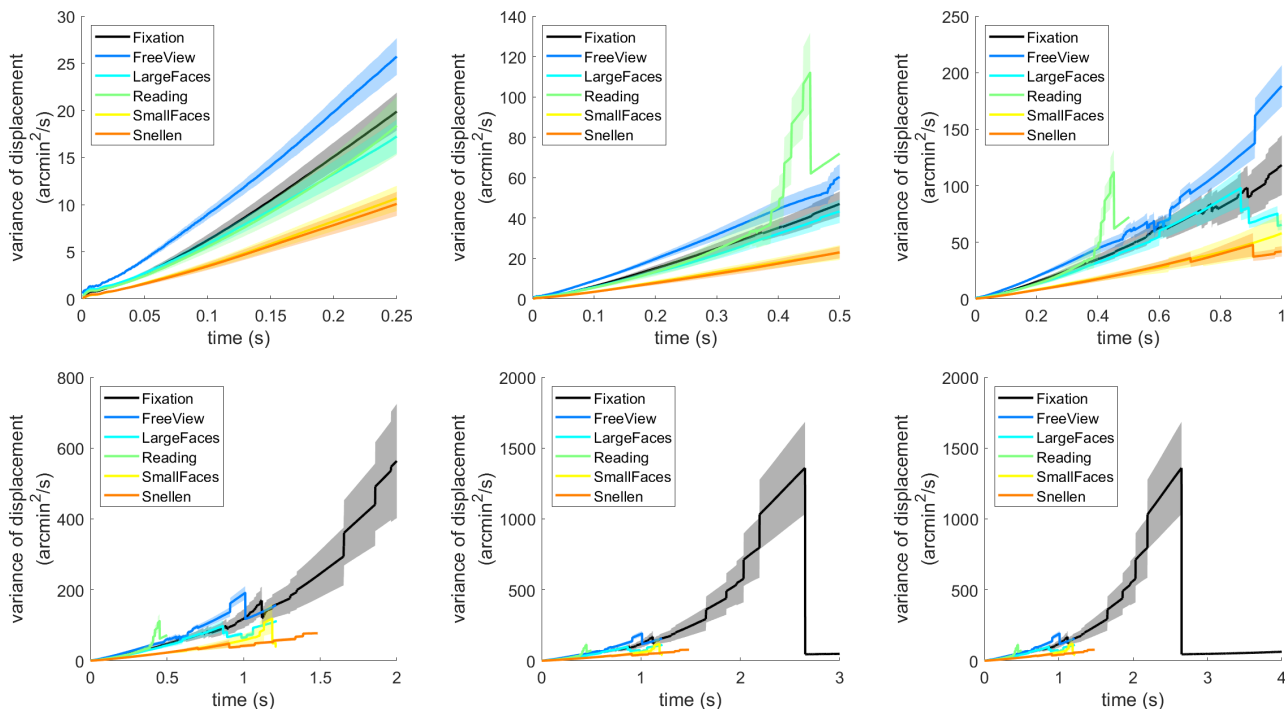


Figure 34: Average variance of displacement by task shown as mean and standard error across subjects. Left panel shows the short time-scale (up to around .25s) and the right panel shows up to 5s. The discontinuities on the longer time-scale are likely the result of shorter trials ending which can drastically change the mean when few data remain.

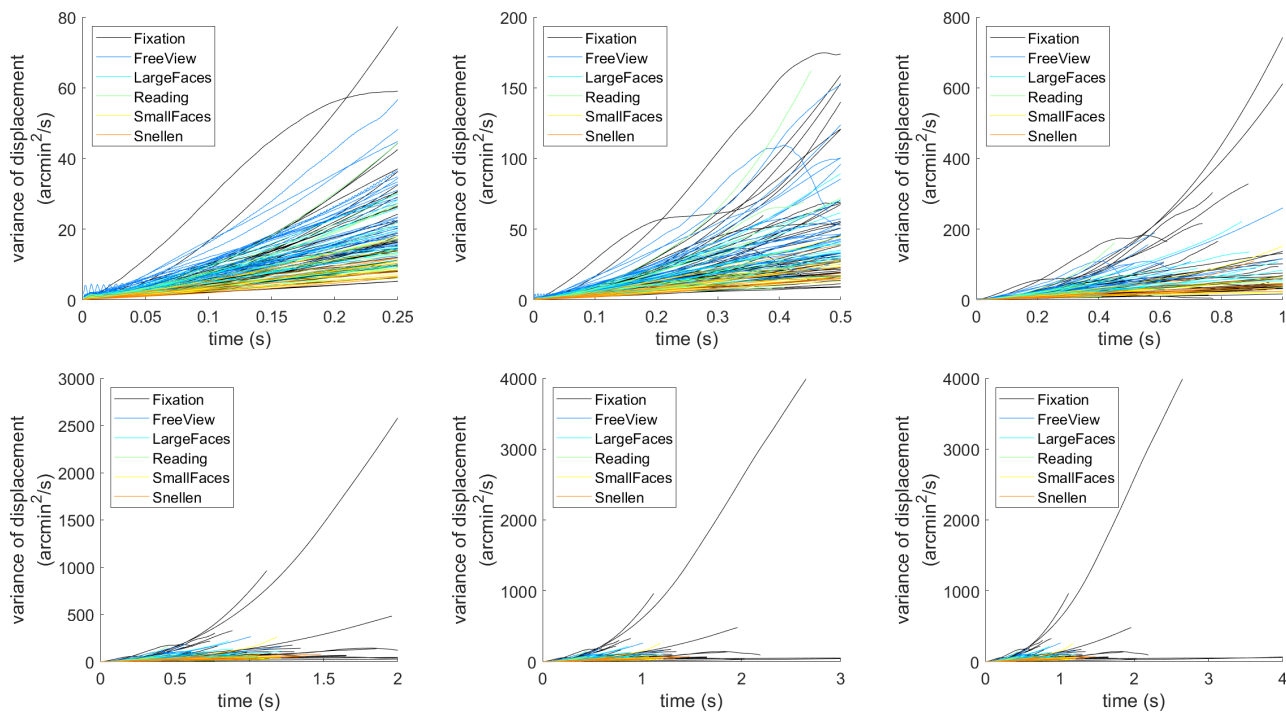


Figure 35: Individual variance of displacement colored by task.

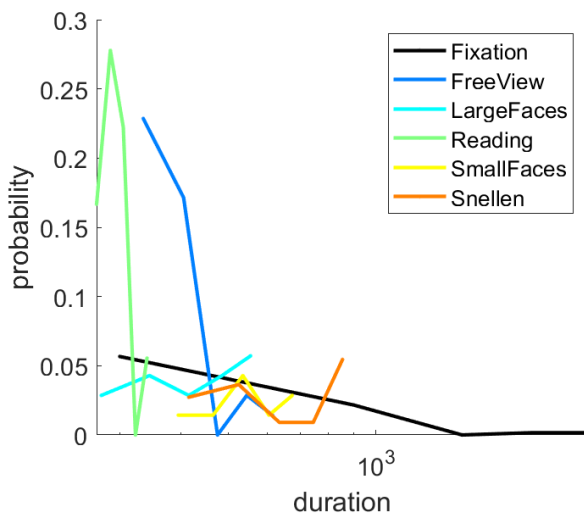


Figure 36: Distribution of drift durations by task. Note that reading and large faces have the shortest durations.

4 Empirical estimations of drift PSD

4.1 Methods

4.1.1 QRad Welch

Power spectra are estimated numerically for given eye traces $x[t]$, $y[t]$ using Welch's method on the signal

$$s[\xi, t, \theta] = e^{-2\pi i(\xi \cos(\theta)x[t] + \xi \sin(\theta)y[t])}$$

where ξ is spatial frequency and θ is the angle in the spectrum. (See Xutao Kuang's note for its derivation and relationship to Q .) Radial averaging (over θ) takes place to compute the spectra as a function of spatial and temporal frequencies:

$$S[\xi, f] = \frac{1}{N} \sum_{n=1}^N \mathcal{F}_t\{s[\xi, t, \theta_n]\}$$

$$P[\xi, f] = |S[\xi, f]|^2$$

4.2 Other considerations

4.2.1 Saturation Regime in Drift - does it exist?

Code in `test_PSD_smoothing.m` in Modeling toolbox.

The goal here is examine whether simulated drifts have a saturation regime as found in saccade PSD. Drifts were simulated as Brownian motion and power spectra computed using the QRad-Welch procedure. Parameters of the simulations:

- Simulated eye traces
 - 4 traces of 10 sec duration
 - variable diffusion constant: 40 or 200 or 1000 arcmin per s²³
 - variable: **if** smoothed, s-golay filter with 41ms window
 - variable: sampling frequency
 - variable: nfft
- Power Spec estimation
 - Hann window (size nfft)
 - spatial frequencies: log scale from 0.1 - 200 cpd
 - power averaged over 30 angles in $[0, 2\pi)$

³a larger diffusion constant makes the effects more striking

4.2.2 Effect of smoothing

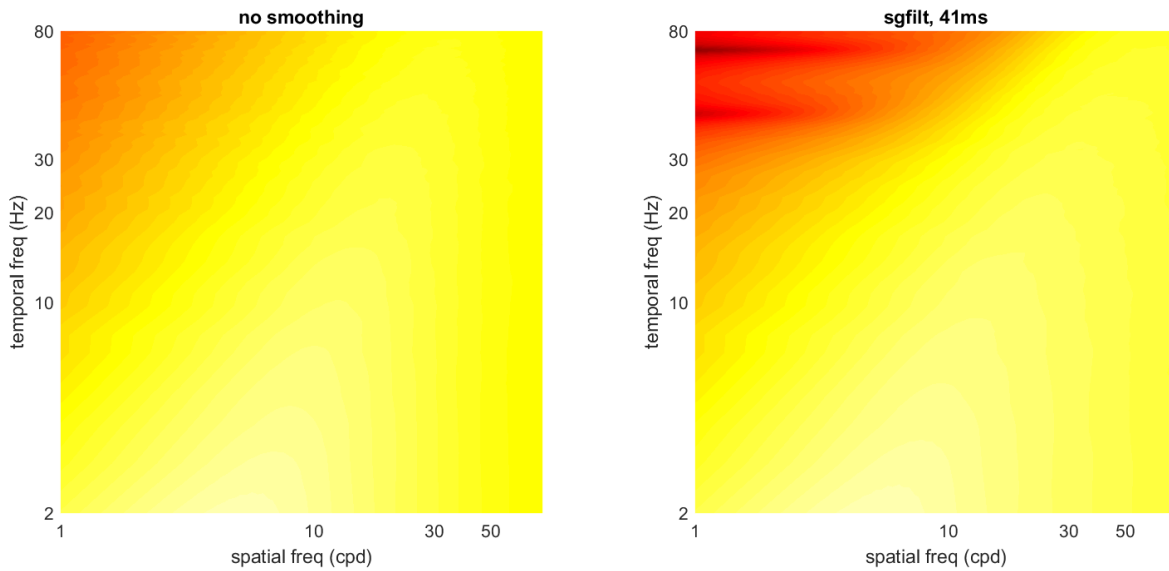


Figure 37: PSD with and without smoothing. Color axes are the same. Slices and parameters are shown in following figure.

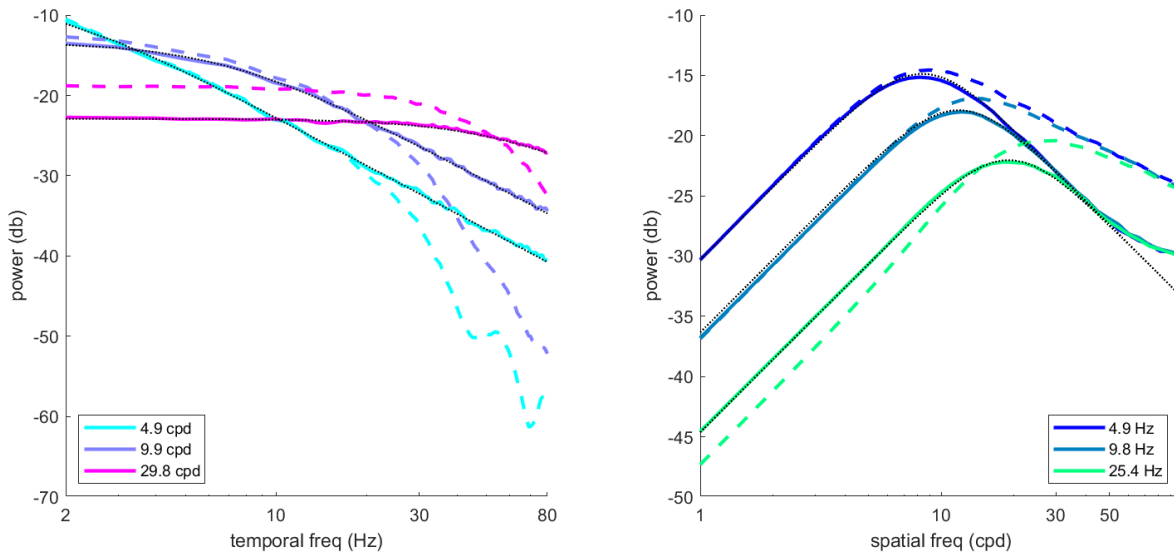


Figure 38: PSD with and without smoothing. Solid lines are *not*-smoothed. Dashed lines are smoothed (s-golay with 41ms window). Dotted black lines are PS from Brownian motion model. LEFT: Slices through a few spatial frequencies. RIGHT: Slices through a few temporal frequencies. $D = 40$; ; Sampling rate 1000Hz; nfft = 1024. Note that smoothing has more impact on high spatial frequencies with this realistic diffusion constant. To make these differences more clear, the next figure uses larger diffusion constants.

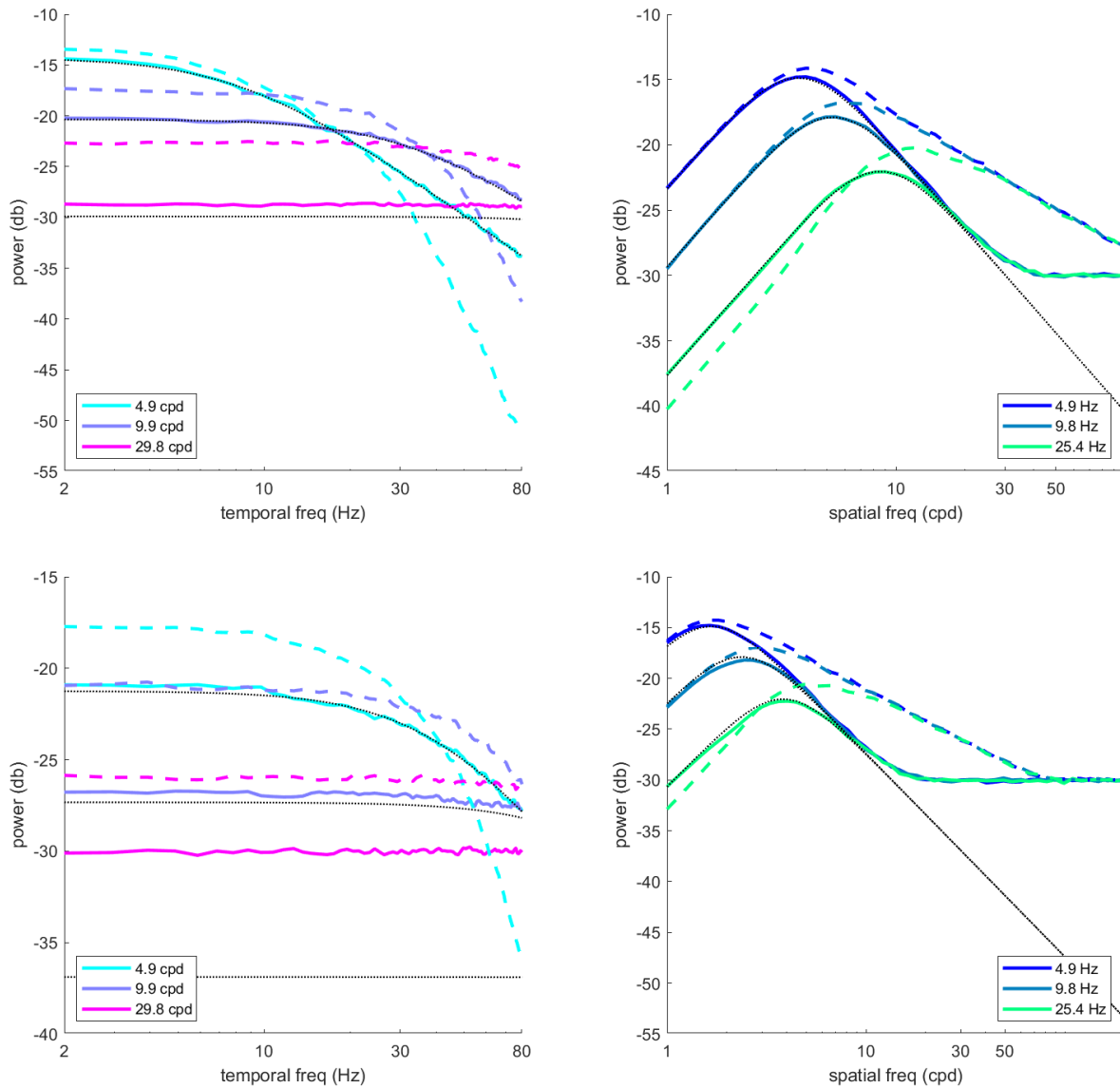


Figure 39: PSD with and without smoothing. Solid lines are *not*-smoothed. Dashed lines are smoothed (s-golay with 41ms window). Dotted black lines are PS from Brownian motion model. LEFT: Slices through a few spatial frequencies. RIGHT: Slices through a few temporal frequencies. TOP: $D = 200$; BOTTOM: $D = 1000$; Sampling rate 1000Hz; nfft = 1024. See list of observations below.

- Smoothing causes the critical frequency to increase slightly relative to not-smoothing and the Brownian motion model.
- Beyond the critical frequency, power drops off more slowly when smoothed.
- As with the Brownian model, power at all temporal frequencies eventually converge, even with smoothing. However, this seems to happen at a higher spatial frequency compared to non-smoothing.

4.2.3 Effect of sampling frequency

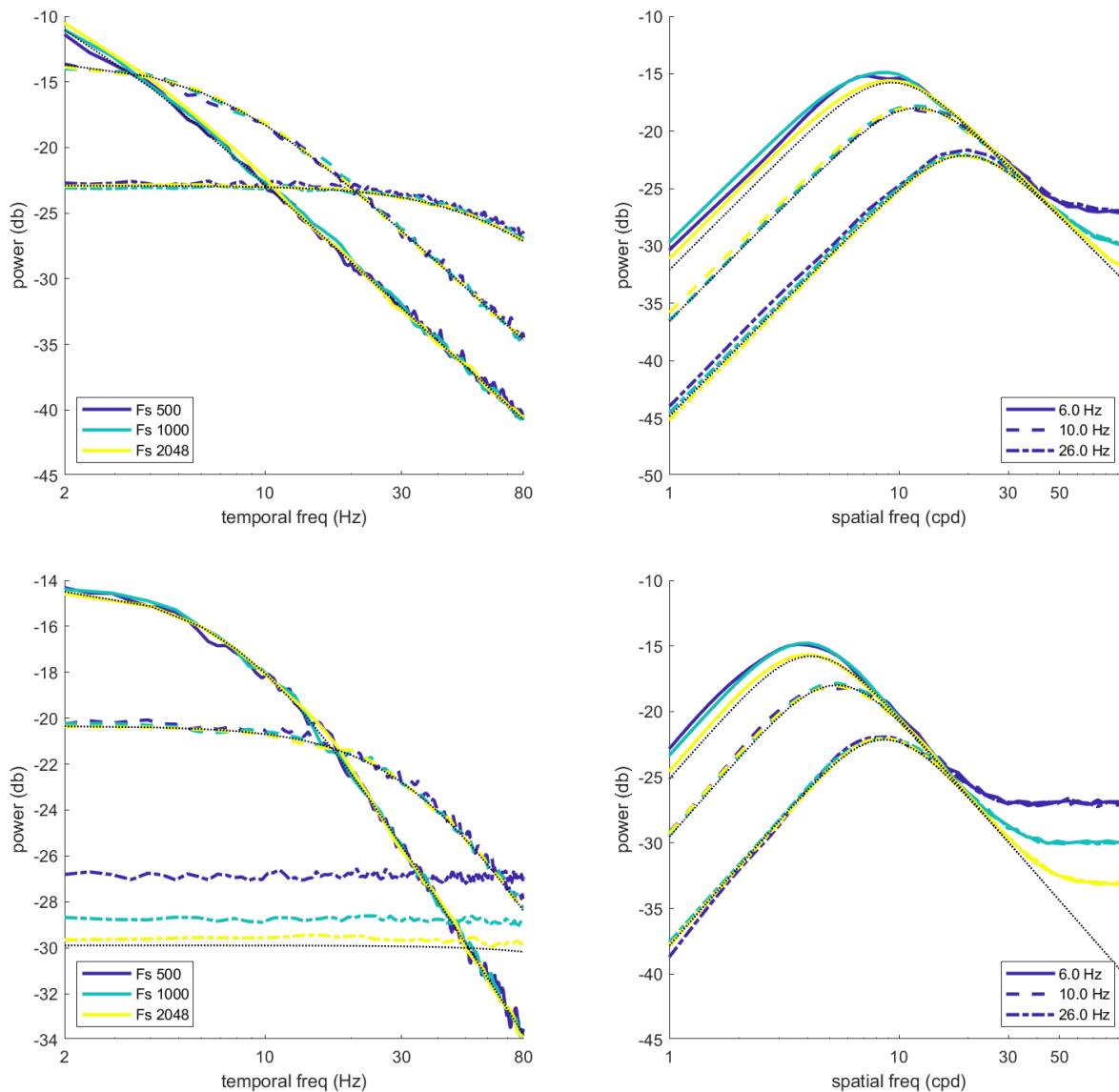


Figure 40: PSD for different sampling frequencies. Different colors mark different sampling frequencies. Different line-styles mark different temporal or spatial frequency slices. Dotted black lines are PS from Brownian motion model. LEFT: Slices through a few spatial frequencies. RIGHT: Slices through a few temporal frequencies. (TOP) $D = 40$, (BOTTOM) $D = 200$; $nfft = 1024$.

- Sampling frequency impacts power at high spatial frequencies (near horizontal lines in left panel).
- The higher sampling frequency pushes the saturation zone to high spatial frequencies (i.e. it matches the Brownian model over a broader range of spatial frequencies).
- The sampling frequency determines the power at which the PSD saturates, but the spatial frequency at which the saturation occurs depends also on the diffusion constant.

5 Appendix

5.1 Additional Derivations & Definitions

5.1.1 Brownian motion: Diffusion Equation & Solutions

A 2-dimensional random walk follows the diffusion equation

$$\frac{\partial q}{\partial t} = D \frac{\partial^2 q}{\partial x^2} + D \frac{\partial^2 q}{\partial y^2}$$

where D is the diffusion constant on each independent dimension. We can also write this as a function of $r^2 = x^2 + y^2$:

$$\begin{aligned} \frac{\partial q}{\partial t} &= D \left[\frac{\partial}{\partial x} \left(\frac{\partial q}{\partial r} \cdot \frac{\partial r}{\partial x} \right) + \frac{\partial}{\partial y} \left(\frac{\partial q}{\partial r} \cdot \frac{\partial r}{\partial y} \right) \right] \\ &= D \left[\underbrace{\frac{\partial}{\partial x} \left(\frac{\partial q}{\partial r} \right)}_{\frac{\partial^2 q}{\partial r^2} \cdot \frac{\partial r}{\partial x}} \cdot \frac{\partial r}{\partial x} + \frac{\partial q}{\partial r} \frac{\partial^2 r}{\partial x^2} + \underbrace{\frac{\partial}{\partial y} \left(\frac{\partial q}{\partial r} \right)}_{\frac{\partial^2 q}{\partial r^2} \cdot \frac{\partial r}{\partial y}} \cdot \frac{\partial r}{\partial y} + \frac{\partial q}{\partial r} \frac{\partial^2 r}{\partial y^2} \right] \\ &= D \left[\frac{\partial^2 q}{\partial r^2} \left(\frac{\partial r}{\partial x} \right)^2 + \frac{\partial^2 q}{\partial r^2} \left(\frac{\partial r}{\partial y} \right)^2 + \frac{\partial q}{\partial r} \left(\frac{\partial^2 r}{\partial x^2} + \frac{\partial^2 r}{\partial y^2} \right) \right] \\ &= D \left[\frac{\partial^2 q}{\partial r^2} \left(\frac{x^2 + y^2}{r^2} \right) + \frac{\partial q}{\partial r} \left(\frac{y^2 + x^2}{r^3} \right) \right] \\ &= D \left[\frac{\partial^2 q}{\partial r^2} + \frac{1}{r} \frac{\partial q}{\partial r} \right] = \frac{D}{r} \frac{\partial}{\partial r} \left(r \frac{\partial q}{\partial r} \right) \end{aligned}$$

$$\begin{aligned} r &= (x^2 + y^2)^{1/2} \\ \frac{\partial r}{\partial x} &= \frac{x}{r} \\ \frac{\partial^2 r}{\partial x^2} &= \frac{r^2 - x^2}{r^3} = \frac{y^2}{r^3} \end{aligned}$$

With the initial condition that at $t = 0$ the particle is concentrated at 0, the diffusion equation is satisfied by

$$\begin{aligned} q(x, y, t; D) &= \frac{1}{4\pi Dt} \exp\left(-\frac{x^2 + y^2}{4Dt}\right) \\ q(r, t; D) &= \frac{1}{4\pi Dt} \exp\left(-\frac{r^2}{4Dt}\right) \end{aligned}$$

Here we confirm that this solves the diffusion equation:

$$\begin{aligned}
\frac{\partial q}{\partial x} &= -\frac{2x}{4Dt}q \\
\frac{\partial^2 q}{\partial x^2} &= -\left(\frac{2}{4Dt}\right)q + \left(\frac{2x}{4Dt}\right)^2 q \\
&= \left(\frac{x^2 - 2Dt}{4D^2t^2}\right)q \\
\frac{\partial^2 q}{\partial x^2} &= \left(\frac{y^2 - 2Dt}{4D^2t^2}\right)q \\
\frac{\partial q}{\partial t} &= \left(-\frac{1}{t} + \frac{x^2 + y^2}{4D^2t^2}\right)q \\
&= \frac{x^2 + y^2 - 4Dt}{4Dt^2}q \\
\Rightarrow D\frac{\partial^2 q}{\partial x^2} + D\frac{\partial^2 q}{\partial y^2} &= \left(\frac{x^2 - 2Dt}{4Dt^2}\right)q + \left(\frac{x^2 - 2Dt}{4Dt^2}\right)q \\
&= \frac{x^2 + y^2 - 4Dt}{4Dt^2}q = \frac{\partial q}{\partial t}
\end{aligned}$$

In three dimensions, the diffusion equation becomes:

$$\begin{aligned}
\frac{\partial q}{\partial t} &= D\frac{\partial^2 q}{\partial x^2} + D\frac{\partial^2 q}{\partial y^2} + D\frac{\partial^2 q}{\partial z^2} \\
\frac{\partial q}{\partial t} &= \frac{D}{r^2}\frac{\partial}{\partial r}\left(r^2\frac{\partial q}{\partial r}\right)
\end{aligned}$$

5.1.2 PSD of Brownian motion

Here we show the steps between $q(x, y, t; D)$ and its transform in frequency space, $Q(\xi_x, \xi_y, f; D)$.

$$\begin{aligned}
q(x, y, t; D) &= \frac{1}{4\pi Dt} \exp\left[-\frac{x^2 + y^2}{4Dt}\right] \\
\tilde{q}(\xi_x, \xi_y, t; D) &= \mathcal{F}_{x,y}\{q(x, y, t; D)\} \\
&= \exp[-4\pi^2 Dt(\xi_x^2 + \xi_y^2)] && \text{see Note 1} \\
Q(\xi_x, \xi_y, f; D) &= \mathcal{F}_t\{\tilde{q}(\xi_x, \xi_y, t; D)\} \\
&= \frac{8\pi^2 D(\xi_x^2 + \xi_y^2)}{16\pi^4 D^2(\xi_x^2 + \xi_y^2)^2 + 4\pi^2 f^2} && \text{see Note 2} \\
&= \frac{2D(\xi_x^2 + \xi_y^2)}{4\pi^2 D^2(\xi_x^2 + \xi_y^2)^2 + f^2}
\end{aligned}$$

Note 1: FT of gaussian is a gaussian with inverse variance

$$\exp[-\pi(a^2x^2 + b^2y^2)] \leftrightarrow \frac{1}{|ab|} \exp\left[-\pi\left(\frac{\xi_x^2}{a^2} + \frac{\xi_y^2}{b^2}\right)\right]$$

Note 2:

$$\exp[-at] \leftrightarrow \frac{2a}{a^2 + 4\pi^2 f^2}$$

5.1.3 Likelihood ratio testing

I compare the two brownian motion models by means of a log likelihood ratio test, a test that can be used to test nested hypotheses (because Brownian motion is a specific type of fractional Brownian motion with $H_{fBM} = 1$.)

I think I made some strange assumptions in this test - namely that the variance of the residuals of the fits vary with time lag. I'm not sure this is valid.

The LLR test statistic (chi-square distribution) is computed as

$$T = 2 \log \left(\frac{\mathcal{L}(H_1)}{\mathcal{L}(H_0)} \right) = \sum_i \frac{(4D_{BM}t_i - \langle r^2 \rangle_i)^2 - (4D_{fBM}t_i^H - \langle r^2 \rangle_i)^2}{\sigma_i^2}$$

where σ_i^2 is computed as the variance across single segment variances of displacements.

5.1.4 OUP for small θ is BM

For small, x , $\exp(x) \approx 1 + x$. Therefore, for small θ , $\exp(-2\theta t) \approx 1 - 2\theta t$ so that

$$\frac{2D}{\theta} (1 + e^{-2\theta t}) \approx \frac{2D}{\theta} (2\theta t) = 4Dt$$

5.2 Additional Figures

5.2.1 H_{fBM} versus D_{fBM} by task

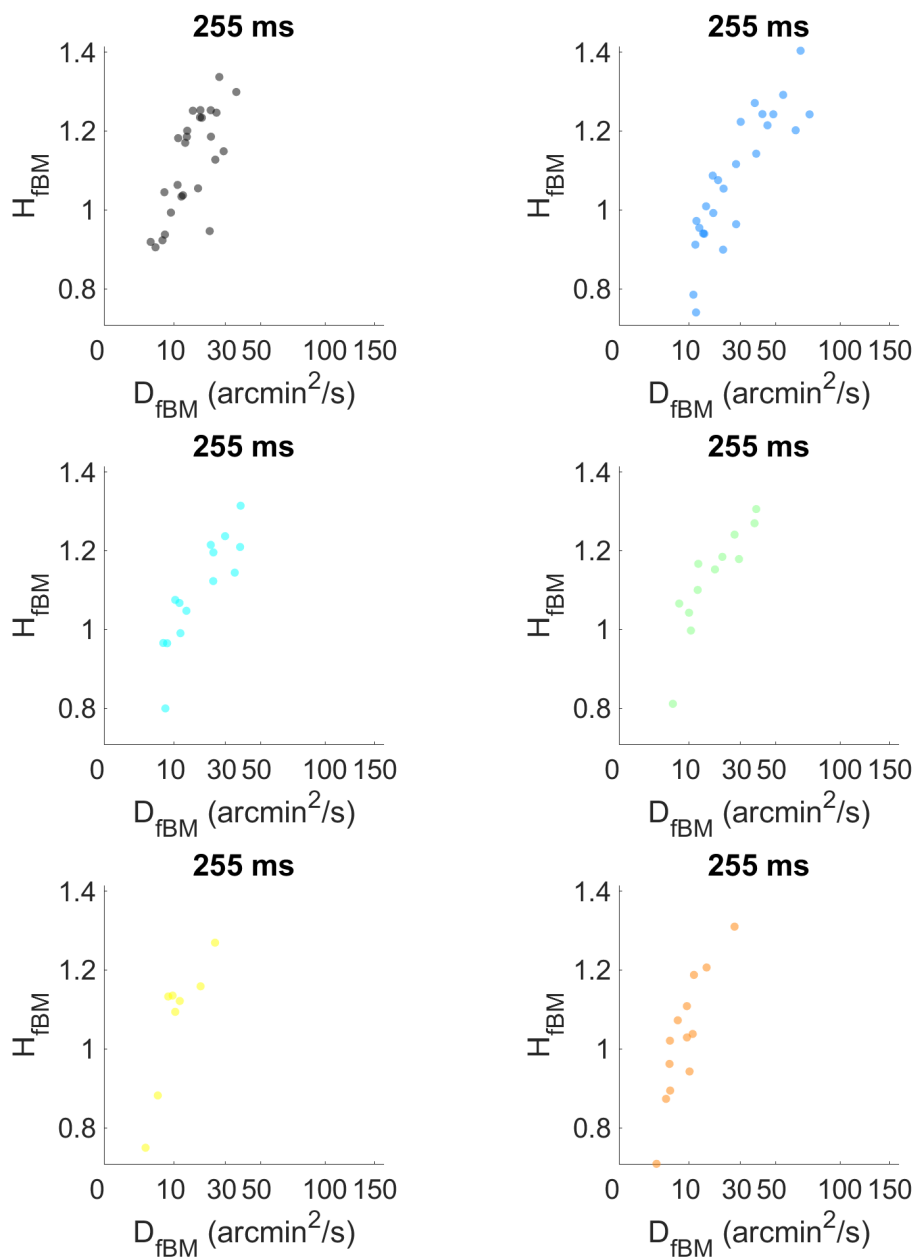


Figure 41: H_{fBM} versus D_{fBM} parameters for fractional brownian motion model separated by task. This is the same data shown in Fig 19. From left-to-right and down the tasks are Fixation, FreeView, Large Faces, Reading, Small Faces, Snellen.

5.3 Data tables

5.3.1 Table of Individual Parameters

All

	255ms					500ms					1000ms				
	D_{BM}	D_{fBM}	H_{fBM}	D_{OUP}	θ_{OUP}	D_{BM}	D_{fBM}	H_{fBM}	D_{OUP}	θ_{OUP}	D_{BM}	D_{fBM}	H_{fBM}	D_{OUP}	θ_{OUP}
mean	16.60	25.41	1.15	16.95	0.17	18.31	24.14	1.10	19.17	0.18	14.86	15.57	1.03	16.27	0.19
STD	10.59	32.85	0.19	10.47	0.48	16.56	35.48	0.24	16.49	0.42	10.35	12.19	0.25	10.15	0.29

Fixation

	255ms					500ms					1000ms				
	D_{BM}	D_{fBM}	H_{fBM}	D_{OUP}	θ_{OUP}	D_{BM}	D_{fBM}	H_{fBM}	D_{OUP}	θ_{OUP}	D_{BM}	D_{fBM}	H_{fBM}	D_{OUP}	θ_{OUP}
Chris	9.27	10.61	1.08	9.28	0.00	9.80	10.39	*1.06	9.80	*0.00					
Matt-	20.60	27.23	1.17	20.59	0.00	25.30	33.82	*1.29	25.29	*0.00					
Thoma	16.56	19.67	1.10	16.54	0.00	16.39	16.46	1.00	16.39	0.00	14.29	12.27	0.74	21.87	0.80
Adria	7.89	9.33	1.10	7.88	0.00	7.90	7.97	1.01	7.90	0.00					
Andre	16.98	34.47	*1.42	16.92	*0.00	14.18	10.96	0.75	21.27	1.19					
Giorg	5.29	5.03	0.97	5.53	0.23	4.76	4.09	0.85	5.84	0.57					
Janis	5.23	4.61	0.93	5.88	0.61	5.45	5.77	1.05	5.46	0.00					
Karis	9.18	11.87	1.15	9.17	0.00	9.65	10.41	1.07	9.65	0.00	9.75	9.89	1.03	9.75	0.00
Kyle-	24.29	42.62	*1.34	24.20	*0.00										
Migue	13.19	20.10	*1.25	13.16	*0.00	13.70	14.45	1.05	13.70	0.00	14.57	15.34	*1.16	14.56	*0.00
A70	7.16	8.13	1.08	7.16	0.00										
AB	19.91	30.48	*1.25	19.88	*0.00										
AO	9.21	9.13	1.00	9.33	0.08										
CH	17.87	29.30	1.30	17.82	0.00										
CS	78.43	302.56	*1.82	78.00	*0.00	132.35	292.27	*1.75	132.22	*0.00					
ML	14.99	19.64	1.16	14.96	0.00	13.01	10.83	0.82	16.90	0.74					
NT	12.85	17.21	1.17	12.83	0.00	12.86	12.85	1.00	13.02	0.03					
SB	9.76	6.67	0.78	12.83	1.52	8.92	7.23	0.81	11.49	0.77					
Bill	28.58	39.95	1.20	28.56	0.00	33.01	39.83	*1.19	33.00	*0.00	33.38	33.64	1.02	33.38	0.00
Claud	6.53	5.71	0.92	7.40	0.66	5.34	3.98	0.72	8.15	1.24	4.32	3.92	*0.72	6.27	*0.54
David	24.65	38.07	1.26	24.60	0.00	27.16	30.84	*1.13	27.15	*0.00	27.04	26.88	0.98	28.32	0.06
Greg	10.45	15.65	1.24	10.43	0.00	12.42	16.15	*1.26	12.42	*0.00	14.45	15.36	*1.19	14.45	*0.00
Joy	9.77	11.24	1.08	9.76	0.00	9.63	9.45	0.98	9.95	0.09	8.92	8.58	0.88	10.56	0.23
Julie	19.41	24.84	1.15	19.37	0.00	23.01	30.46	*1.28	23.00	*0.00	27.43	29.57	*1.23	27.42	*0.00
Katha	10.38	15.04	*1.22	10.36	*0.00	10.61	10.77	1.01	10.65	0.01	9.91	9.66	0.92	11.06	0.15
Kulve	10.32	13.50	1.16	10.32	0.00	11.02	12.12	1.09	11.02	0.00	11.54	11.79	1.06	11.54	0.00
Laure	12.03	13.31	1.06	12.04	0.00	11.72	11.34	0.97	12.32	0.13	10.96	10.63	0.91	12.39	0.17
Maria	13.02	22.02	*1.31	13.00	*0.00	15.33	19.55	*1.24	15.32	*0.00	13.17	11.94	0.72	21.82	0.76
Wende	8.77	6.86	0.85	10.58	1.02	7.71	6.67	0.86	9.08	0.45					
mean	15.61	28.10	1.16	15.81	0.14	18.38	26.19	1.05	19.21	0.22	15.36	15.34	0.97	17.18	0.21
STD	13.52	53.92	0.20	13.33	0.36	25.30	57.49	0.22	25.07	0.39	8.53	8.96	0.17	8.46	0.30

FreeView

	255ms					500ms					1000ms				
	D_{BM}	D_{fBM}	H_{fBM}	D_{OUP}	θ_{OUP}	D_{BM}	D_{fBM}	H_{fBM}	D_{OUP}	θ_{OUP}	D_{BM}	D_{fBM}	H_{fBM}	D_{OUP}	θ_{OUP}
Charl	20.63	17.26	0.89	23.51	0.68	20.61	20.79	1.01	20.63	0.00	25.21	28.10	1.35	25.21	0.00
Clair	31.51	44.32	1.20	31.43	0.00										
DaveF	28.70	83.06	*1.64	28.58	*0.00	43.14	76.03	*1.57	43.11	*0.00					
DaveV	16.91	30.51	*1.35	16.85	*0.00	17.04	17.05	1.00	17.54	0.08					
Ignat	51.31	93.02	*1.36	51.18	*0.00										
Jonat	29.08	27.55	0.97	30.19	0.19	26.37	22.04	0.83	34.07	0.72					
Jonat	26.74	26.93	1.00	26.76	0.00	26.56	25.25	0.95	28.77	0.22					
Julie	44.00	51.60	1.09	43.90	0.00	45.72	51.15	1.10	45.69	0.00					
Julie	29.75	40.47	1.18	29.66	0.00	29.74	29.28	0.98	30.89	0.10					
Laure	30.43	43.13	1.21	30.37	0.00	37.63	53.18	*1.34	37.62	*0.00	53.82	63.85	*1.56	53.82	*0.00
Laure	29.10	33.85	1.09	29.05	0.00										
Roshn	18.32	23.18	1.14	18.33	0.00	22.86	34.08	*1.40	22.86	*0.00					
RyanF	18.31	18.02	0.99	18.87	0.15	17.16	14.86	0.86	21.27	0.60					
RyanV	15.98	14.65	0.95	17.18	0.38	14.66	12.67	0.86	17.92	0.56					
SamFV	22.52	29.54	1.16	22.48	0.00	23.52	24.20	1.03	23.51	0.00					
SamVS	21.39	33.20	1.26	21.35	0.00										
Teale	19.09	14.50	0.84	23.26	1.08	17.50	15.15	0.86	20.99	0.50					
Teale	19.87	22.42	1.07	19.86	0.00										
XixiF	15.11	16.95	1.07	15.12	0.00										
XixiV	13.12	9.95	0.84	16.53	1.25										
Andre	10.37	6.35	0.71	15.27	2.19										
Deniz	19.51	37.69	*1.39	19.49	*0.00	29.16	55.76	*1.65	29.14	*0.00					
Laird	32.21	66.23	*1.43	32.13	*0.00	48.95	98.52	*1.71	48.92	*0.00					
Laura	15.82	18.74	1.10	15.81	0.00										
Manue	18.87	23.25	1.12	18.88	0.00	20.44	23.32	1.13	20.44	0.00					
Marc	22.36	22.29	1.00	23.27	0.19	21.63	19.78	0.92	24.53	0.38					
Melis	32.43	48.72	1.24	32.39	0.00	34.41	43.68	*1.18	34.40	*0.00					
Miche	16.16	11.42	0.79	20.97	1.44	11.29	6.43	*0.49	25.62	*2.85					
mean	23.91	32.46	1.11	24.74	0.27	26.76	33.85	1.10	28.84	0.32	39.52	45.98	1.45	39.51	0.00
STD	9.23	21.02	0.21	8.59	0.55	10.80	23.82	0.31	9.51	0.66	20.23	25.28	0.15	20.23	0.00

LargeFaces

	255ms					500ms					1000ms				
	D_{BM}	D_{fBM}	H_{fBM}	D_{OUP}	θ_{OUP}	D_{BM}	D_{fBM}	H_{fBM}	D_{OUP}	θ_{OUP}	D_{BM}	D_{fBM}	H_{fBM}	D_{OUP}	θ_{OUP}
Andre	10.80	13.73	1.14	10.80	0.00	12.98	17.28	*1.28	12.98	*0.00	14.38	16.27	*1.23	14.38	*0.00
Brand	8.97	12.67	1.21	8.97	0.00	9.17	8.85	0.96	10.00	0.24					
Chris	9.62	12.16	1.14	9.63	0.00										
Dylan	9.95	15.14	1.25	9.94	0.00	13.16	21.28	*1.48	13.16	*0.00					
Kavi-	14.18	20.65	1.22	14.18	0.00	16.23	19.64	*1.19	16.23	*0.00					
Kyle-	24.10	58.46	*1.53	24.03	*0.00	36.93	70.34	*1.65	36.91	*0.00					
Matt-	24.97	30.23	1.11	24.94	0.00	28.39	35.39	*1.22	28.38	*0.00					
Mia-5	15.68	16.58	1.03	15.66	0.00										
Patri	16.60	19.85	1.11	16.58	0.00	17.64	18.93	1.07	17.63	0.00	18.37	19.30	*1.15	18.37	*0.00
Rolli	18.98	21.66	1.08	18.97	0.00	20.36	22.13	1.08	20.36	0.00	17.63	16.43	0.80	24.45	0.47
Sande	28.16	39.64	1.20	28.12	0.00	32.58	40.92	*1.23	32.57	*0.00					
Sidha	13.33	16.93	1.14	13.34	0.00										
Thoma	13.19	15.02	1.08	13.20	0.00	14.01	15.79	1.12	14.00	0.00					
Tracy	20.23	25.32	1.13	20.19	0.00	20.64	20.93	1.01	20.64	0.00					
mean	16.34	22.72	1.17	16.32	0.00	20.19	26.50	1.21	20.26	0.02	16.79	17.34	1.06	19.07	0.16
STD	6.15	12.78	0.12	6.13	0.00	8.86	17.04	0.20	8.75	0.07	2.12	1.70	0.23	5.07	0.27

Reading

	255ms					500ms					1000ms				
	D_{BM}	D_{fBM}	H_{fBM}	D_{OUP}	θ_{OUP}	D_{BM}	D_{fBM}	H_{fBM}	D_{OUP}	θ_{OUP}	D_{BM}	D_{fBM}	H_{fBM}	D_{OUP}	θ_{OUP}
Audre	16.79	20.61	1.12	16.77	0.00										
Avrey	18.24	45.99	*1.56	18.20	*0.00	29.66	59.91	*1.71	29.64	*0.00					
Chris	7.95	15.31	*1.39	7.94	*0.00										
Cody	13.56	12.67	0.96	14.16	0.23										
Kevin	9.62	11.04	1.08	9.62	0.00										
Matt	24.04	44.63	*1.37	24.00	*0.00										
Mia	9.54	7.99	0.90	11.06	0.79										
Olivi	36.52	118.08	*1.71	36.36	*0.00										
Orian	9.61	12.23	1.14	9.60	0.00										
Patri	23.59	45.07	*1.39	23.53	*0.00										
Rolli	7.14	3.77	*0.62	12.37	*3.24										
Tracy	12.00	17.48	1.22	12.00	0.00										
Victo	26.51	53.61	*1.42	26.43	*0.00										
mean	16.55	31.42	1.22	17.08	0.33	29.66	59.91	1.71	29.64	0.00	NaN	NaN	NaN	NaN	NaN
STD	8.87	31.08	0.29	8.35	0.90	0.00	0.00	0.00	0.00	0.00	NaN	NaN	NaN	NaN	NaN

SmallFaces

	255ms					500ms					1000ms				
	D_{BM}	D_{fBM}	H_{fBM}	D_{OUP}	θ_{OUP}	D_{BM}	D_{fBM}	H_{fBM}	D_{OUP}	θ_{OUP}	D_{BM}	D_{fBM}	H_{fBM}	D_{OUP}	θ_{OUP}
Adria	6.98	9.36	*1.17	6.97	*0.00	7.73	8.76	*1.12	7.73	*0.00					
Andre	10.05	15.62	1.26	10.03	0.00	11.85	15.07	*1.24	11.85	*0.00	12.93	13.21	*1.07	12.93	*0.00
Giorg	8.48	13.37	1.27	8.47	0.00	8.72	8.61	0.99	9.20	0.14	6.31	5.49	0.61	12.35	1.06
Janis	6.34	6.75	1.04	6.35	0.00	6.64	6.89	1.04	6.64	0.00	5.95	5.76	0.90	6.70	0.16
Karis	8.26	9.86	1.11	8.26	0.00	8.61	9.02	1.05	8.61	0.00	8.49	8.54	1.02	8.49	0.00
Kerri	16.42	28.27	*1.33	16.37	*0.00	20.26	27.89	*1.32	20.25	*0.00	29.05	35.48	*1.67	29.05	*0.00
Kyle-	14.12	15.49	1.05	14.09	0.00	13.82	13.41	0.97	14.41	0.11					
Migue	10.31	14.72	1.21	10.30	0.00	11.26	12.97	*1.14	11.26	*0.00	14.35	16.17	*1.38	14.35	*0.00
mean	10.12	14.18	1.18	10.11	0.00	11.11	12.83	1.11	11.24	0.03	12.85	14.11	1.11	13.98	0.20
STD	3.51	6.55	0.11	3.49	0.00	4.39	6.72	0.12	4.41	0.06	8.65	11.28	0.37	7.93	0.42

Snellen

	255ms					500ms					1000ms				
	D_{BM}	D_{fBM}	H_{fBM}	D_{OUP}	θ_{OUP}	D_{BM}	D_{fBM}	H_{fBM}	D_{OUP}	θ_{OUP}	D_{BM}	D_{fBM}	H_{fBM}	D_{OUP}	θ_{OUP}
A024-	6.50	6.05	0.96	6.94	0.33	6.28	5.75	0.91	7.16	0.36					
A039-	6.40	7.19	1.07	6.40	0.00	6.02	5.34	0.88	7.18	0.49	4.91	4.56	*0.79	6.50	*0.40
A068-	10.05	9.11	0.94	11.22	0.56	9.43	8.46	0.89	10.95	0.41	8.61	8.28	0.88	9.99	0.20
A083-	10.98	13.33	1.12	10.97	0.00	12.60	15.76	*1.22	12.60	*0.00					
A084-	5.50	5.48	1.00	5.49	0.00	5.62	5.65	1.01	5.62	0.00					
Anne-	5.13	3.84	0.83	6.41	1.21	4.28	3.24	*0.73	6.28	*1.12	3.41	3.08	*0.70	5.16	*0.61
MAC-d	6.97	7.18	1.02	6.97	0.00	7.18	7.72	1.07	7.18	0.00					
A70	5.82	8.67	*1.24	5.81	*0.00	7.33	10.50	*1.36	7.33	*0.00	9.45	10.54	*1.35	9.45	*0.00
AB	11.87	12.23	1.02	11.89	0.00	11.67	11.36	0.97	12.15	0.11	11.20	11.01	0.95	11.97	0.09
AO	7.97	8.94	1.07	7.96	0.00	7.75	7.59	0.98	7.98	0.08	6.92	6.48	0.81	9.26	0.42
CH	10.07	11.69	1.09	10.06	0.00	11.94	16.56	1.33	11.93	0.00					
CS	6.51	8.10	1.13	6.50	0.00	7.15	8.25	1.14	7.15	0.00					
ML	10.90	17.62	*1.29	10.89	*0.00	13.10	17.36	*1.28	13.10	*0.00	14.99	15.76	*1.16	14.98	*0.00
NT	8.06	10.16	1.14	8.05	0.00	8.85	10.38	*1.16	8.84	*0.00	9.88	10.36	*1.15	9.88	*0.00
SB	16.01	25.27	*1.27	15.97	*0.00	18.49	22.80	*1.21	18.48	*0.00					
mean	8.58	10.32	1.08	8.77	0.14	9.18	10.45	1.08	9.60	0.17	8.67	8.76	0.97	9.65	0.21
STD	3.02	5.38	0.13	2.95	0.34	3.75	5.44	0.18	3.51	0.31	3.65	4.06	0.22	3.03	0.23

5.3.2 Compare Model Paramaters by Task

100ms	255ms	500ms	750ms	1000ms
D_{BM}				
ANOVA F(101, 5) =14.10, $p=1.890e-10$	ANOVA F(101, 5) =6.30, $p=3.952e-05$	ANOVA F(72, 5) =2.56, $p=3.447e-02$	ANOVA F(41, 4) =6.45, $p=4.032e-04$	ANOVA F(27, 4) =5.99, $p=1.381e-03$
Fixation : FreeView : 1.043e-06	Fixation : FreeView : 1.590e-02	FreeView : Snellen : 2.245e-02	Fixation : FreeView : 4.207e-02	Fixation : FreeView : 4.336e-03
FreeView : LargeFaces : 2.700e-03	FreeView : SmallFaces : 5.776e-03		FreeView : SmallFaces : 2.857e-02	FreeView : LargeFaces : 3.462e-02
FreeView : Reading : 6.054e-04	FreeView : Snellen : 2.770e-05		FreeView : Snellen : 2.356e-03	FreeView : SmallFaces : 3.299e-03
D_{fBM}				
ANOVA F(101, 5) =1.51, $p=1.931e-01$	ANOVA F(101, 5) =1.24, $p=2.979e-01$	ANOVA F(72, 5) =1.13, $p=3.508e-01$	ANOVA F(41, 4) =5.62, $p=1.064e-03$	ANOVA F(27, 4) =6.41, $p=9.195e-04$
H_{fBM}				
ANOVA F(101, 5) =1.84, $p=1.123e-01$	ANOVA F(101, 5) =1.07, $p=3.842e-01$	ANOVA F(72, 5) =2.11, $p=7.438e-02$	ANOVA F(41, 4) =1.77, $p=1.540e-01$	ANOVA F(27, 4) =2.09, $p=1.097e-01$
D_{OUP}				
ANOVA F(101, 5) =16.62, $p=5.998e-12$	ANOVA F(101, 5) =7.41, $p=5.882e-06$	ANOVA F(72, 5) =3.17, $p=1.215e-02$	ANOVA F(41, 4) =6.35, $p=4.522e-04$	ANOVA F(27, 4) =5.95, $p=1.442e-03$
Fixation : FreeView : 3.319e-08	Fixation : FreeView : 5.037e-03	FreeView : Snellen : 7.190e-03	Fixation : FreeView : 4.600e-02	Fixation : FreeView : 7.807e-03
FreeView : LargeFaces : 3.784e-04	FreeView : SmallFaces : 1.783e-03		FreeView : SmallFaces : 3.384e-02	FreeView : SmallFaces : 4.305e-03
FreeView : Reading : 5.129e-05	FreeView : Snellen : 5.532e-06		FreeView : Snellen : 2.832e-03	FreeView : Snellen : 5.122e-04
θ_{OUP}				
ANOVA F(101, 5) =0.41, $p=8.416e-01$	ANOVA F(101, 5) =1.11, $p=3.614e-01$	ANOVA F(72, 5) =0.98, $p=4.369e-01$	ANOVA F(41, 4) =1.46, $p=2.312e-01$	ANOVA F(27, 4) =0.23, $p=9.167e-01$

Table 3: ANOVA to compare effect of task on model parameters and p -values from multiple comparisons. Only pairs of tasks with significant differences are listed.